INTERACTION NOTES

Note 190

July 1970

COMPUTATION OF GREEN'S FUNCTIONS
FOR BODIES OF REVOLUTION
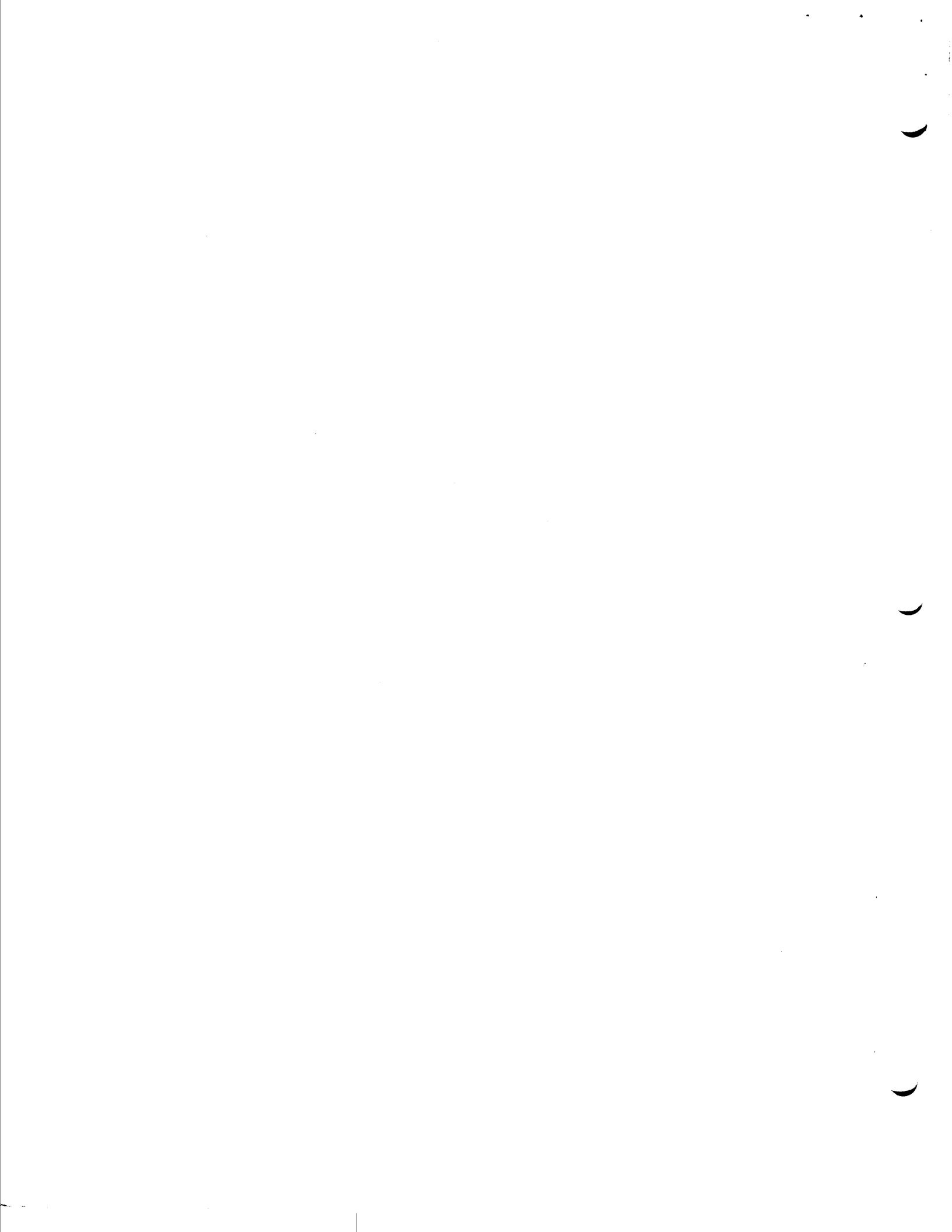
by

Roger F. Harrington
Joseph R. Mautz

Electrical Engineering Department
Syracuse University
Syracuse, New York

ABSTRACT

Computer programs are developed to calculate the electric field intensity at one point in space due to an electric dipole at another point in space, in the vicinity of a conducting body of revolution. The programs are valid both external and internal to the conducting surface. Hence, they may be used to compute not only radiated and scattered fields, but also fields internal to resonant cavities. The current on the conducting body is computed as an intermediary step in the program. The solution is obtained by the method of moments applied to the potential integral equation, and involves inversion of the generalized impedance matrix. The principal limitations to the solution are due to the matrix computation and inversion, which requires that the generating contour be at most several wavelengths long. Some examples of computations for spheres, disks, and cone-spheres are given to illustrate the programs.

CONTENTS

I. INTRODUCTION

For this report, we define the Green's function to be the electric field intensity at one point in space due to an electric current element at another point, subject to specified boundary conditions on a surface of revolution. This Green's function is in general a dyadic, requiring nine components to specify it completely [1]. We compute one component at a time by specifying the field component desired and the current element orientation. The boundary conditions are usually taken to be vanishing tangential electric field on the surface of revolution (perfect electric conductor), but any other impedance boundary condition can be treated by considering the surface to be a loaded body [2].

A solution is effected by applying the method of moments to the potential integral equation for the problem [3]. The solution is expressed in terms of generalized network parameters, for which computer programs are available [4]. The free-space field from the current element is taken as the impressed field over the body of revolution, and the current on the body is computed as in a scattering problem. The electric field component at another point in space is computed by reciprocity. This involves placing a second current element at the field point and evaluating its reaction with the current on the body of revolution [5].

The computer programs of this report are valid for current elements both outside and inside of closed bodies of revolution. Hence, they are valid for both radiation problems and electromagnetic resonators. They can be used to compute the behavior of more complicated sources, such as antenna elements and arrays, by superimposing the contributions due to all elements of the source. They can be used to rigorously solve such problems as wire antennas on bodies of revolution, by using the Green's function as the kernel of the integral equation which treats the body of revolution as part of the environment.

II. METHOD OF SOLUTION

Figure 1 represents the geometry of the general problem. At r_c there exists a current element $I\ell$ in the direction u_c, producing a free-space "incident" field E^i. Over the surface S there exists a current J which produces a free-space "scattered" field E^s. A general impedance boundary condition at the surface S can be represented by

$$E^i_{tan} + E^s_{tan} = \mathcal{Z}(J) \tag{1}$$

where $\mathcal{Z}$ is an impedance function and the subscripts "tan" denote tangential components. A perfect conductor over S is represented by the case $\mathcal{Z} = 0$. It is desired to obtain the component in the direction u_f of the total electric field $E = E^i + E^s$ at the point r_f.

The incident field E^i can be calculated for the source $I\ell$, and hence is the known quantity in (1). The scattered field E^s can be related to the current J on S by the potential integral solution, a linear operation which we represent by

$$- E^s_{tan} = L(J) \tag{2}$$

Substituting (2) into (1) and rearranging, we have

$$L(J) + \mathcal{Z}(J) = E^i_{tan} \tag{3}$$

The solution for the unknown current J on S is represented by

$$J = (L + \mathcal{Z})^{-1} E^i_{tan} \tag{4}$$

where $(L + \mathcal{Z})^{-1}$ is the operator inverse to the $L + \mathcal{Z}$ of (3).

Instead of the current J, we ultimately want the field component

$$E_f = u_f \cdot (E^i + E^s) \tag{5}$$

at r_f. The term $u_f \cdot E^i$ is easily calculated because it is the free-space field due to $I\ell$ at r_c. To evaluate $u_f \cdot E^s$ we use the reciprocity relationship [3]
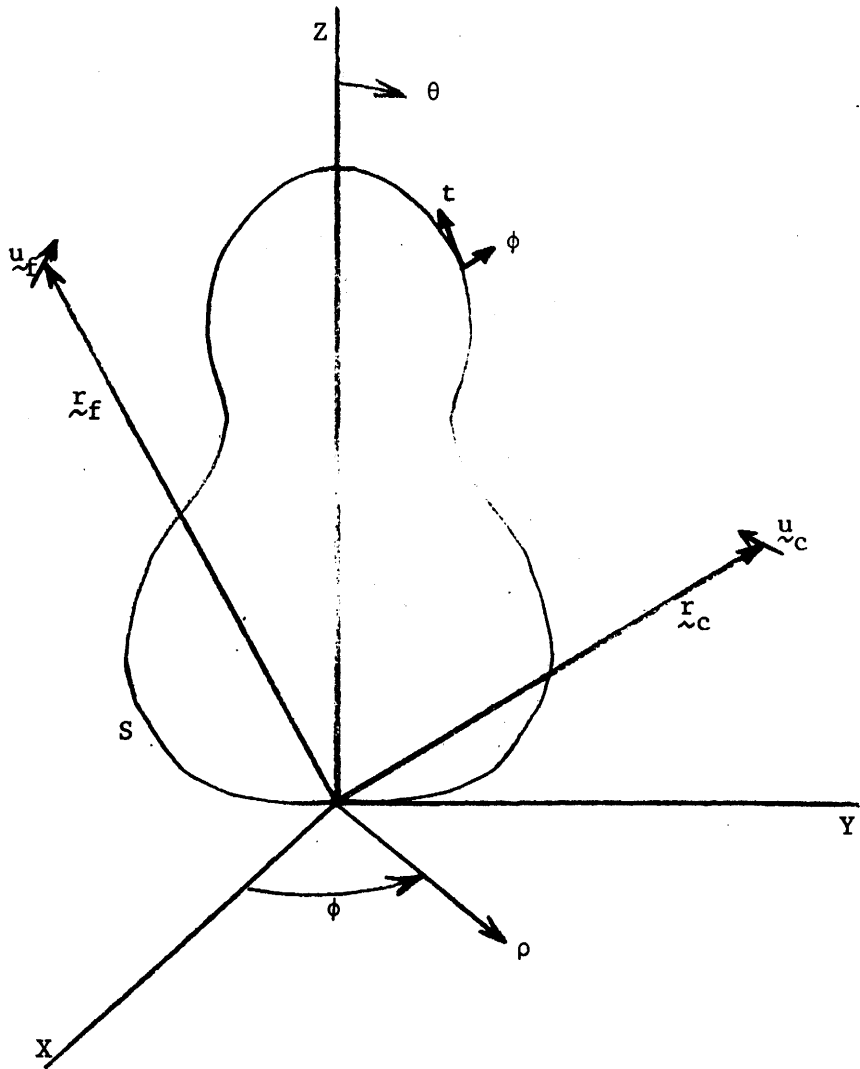
Figure 1. Geometry and coordinate system.

$$\underset{\sim}{u}_f \cdot \underset{\sim}{E}^s = K(r_f) \iint\limits_S \underset{\sim}{E}^i_f \cdot \underset{\sim}{J} \, ds \tag{6}$$

where

$$K(r_f) = \frac{\omega\mu \, e^{-jkr_f}}{j4\pi \, r_f} \tag{7}$$

and $\underset{\sim}{E}^i_f$ is the incident field produced by a current element $I\underset{\sim}{\ell}_f$ placed at $\underset{\sim}{r}_f$ in the direction $\underset{\sim}{u}_f$ and of amplitude such that it produces a unit field at the origin. The surface integral in (6) is a bilinear functional which we denote by

$$<A,B> = \iint\limits_S \underset{\sim}{A} \cdot \underset{\sim}{B} \, ds \tag{8}$$

Substituting from (4) and (8) into (6), we now have

$$\underset{\sim}{u}_f \cdot \underset{\sim}{E}^s = K(r_f) <E^i_f, (L + \mathcal{J})^{-1} E^i_c> \tag{9}$$

where $\underset{\sim}{E}^i_c = \underset{\sim}{E}^i_{tan}$. This last change in notation is introduced to emphasize that $\underset{\sim}{E}^i_f$ and $\underset{\sim}{E}^i_c$ are similar quantities, differing only in the position of the current element.

The inverse operator $(L + \mathcal{J})^{-1}$ is usually not known exactly, and we employ the method of moments to obtain an approximate solution [3]. The details of this are given in previous reports [2,4], and we here give only the results. Let $\{J_i \mid i = 1,2,\ldots, N\}$ represent a set of current expansion functions, and $\{W_i \mid i = 1,2,\ldots, N\}$ represent a set of testing functions. A matrix solution which approximates (9) is then

$$\underset{\sim}{u}_f \cdot \underset{\sim}{E}^s = K(r_f)[\widetilde{V}_f][Z + Z_L]^{-1}[V_c] \tag{10}$$

where $[V_f]$ and $[V_c]$ are the column matrices

$$[V_f] = [<E^i_f, J_n>] \tag{11}$$

$$[V_c] = [<W_m, E^i_c>] \tag{12}$$

6

and [Z] and [Z_L] are the square matrices

$$[Z] = [<W_m, LJ_n>] \qquad (13)$$

$$[Z_L] = [<W_m, \partial J_n>] \qquad (14)$$

A computer program is available for (13) for bodies of revolution [4]. If ∂ is a simple function of position on S, then (14) is easily calculated. For the remainder of this report, we assume S to be a perfect conductor, in which case [Z_L] = 0. The computation of [V_c] and [V_f] can be effected by the programs of this report. The mathematical details of the solution are given in Section V. The computer programs and instructions for running them are given in Sections VI and VII.

III. REPRESENTATIVE COMPUTATIONS

Some representative computations made with the programs of Section VII are given here both to demonstrate the accuracy obtainable and to illustrate the types of problems that can be run. The first checks were made by comparing the general program computations with the exact modal solutions for spheres. Figure 2 shows the results of one such computation. It consists of plots of the radiation gain patterns[*] for incremental electric dipoles adjacent to a conducting sphere. Each graph shows the three cases (1) r-directed dipole, (2) θ-directed dipole and (3) φ-directed dipole. The sphere is λ/2 in diameter and the dipole is λ/4 from the sphere's surface. Three cases are shown, (a) dipole positioned on the z-axis, (b) dipole positioned along an axis rotated 45° from the z-axis, and (c) dipole positioned on the equatorial plane. The results using the general program and those using the exact solution were so close that no differences show in Figure 2. Computation of the error in gain (exact minus computed) was in all cases less than ±0.02, and oscillated

---

[*]All radiation patterns are in the φ=0 plane.

(a) $\theta_0 = 0$

(b) $\theta_0 = \pi/4$

r - directed $I\ell$ ....

θ - directed $I\ell$ -----------

ϕ - directed $I\ell$ —————

(c) $\theta_0 = \pi/2$
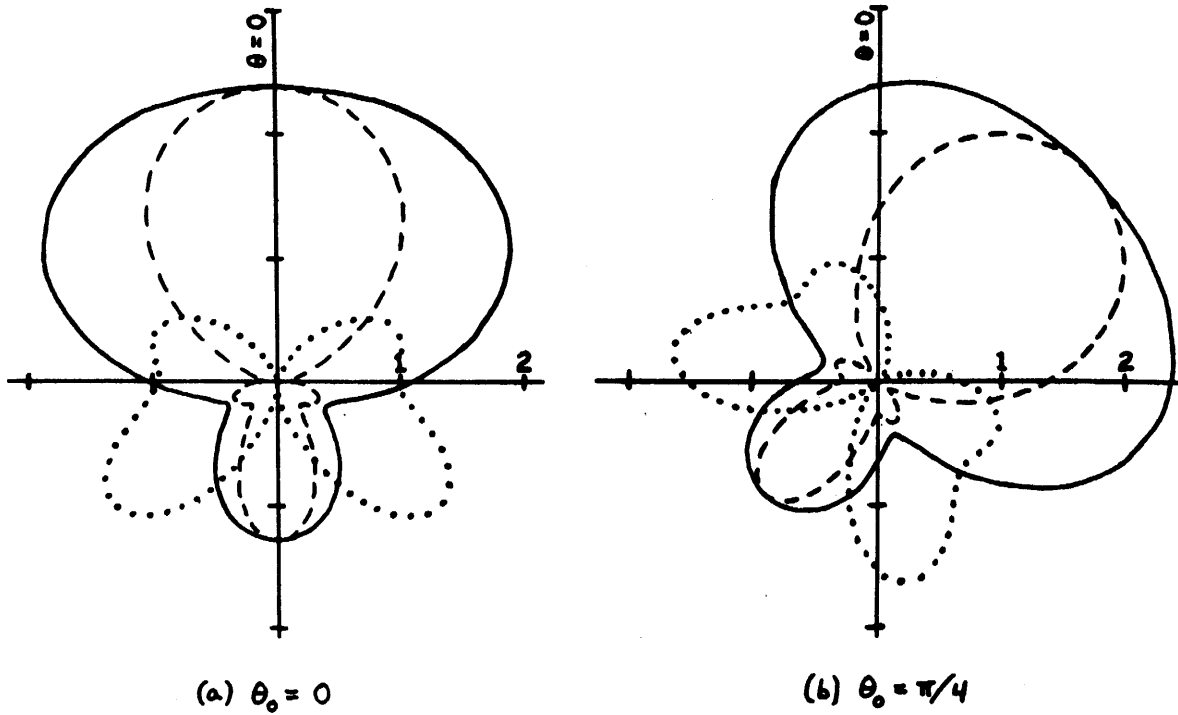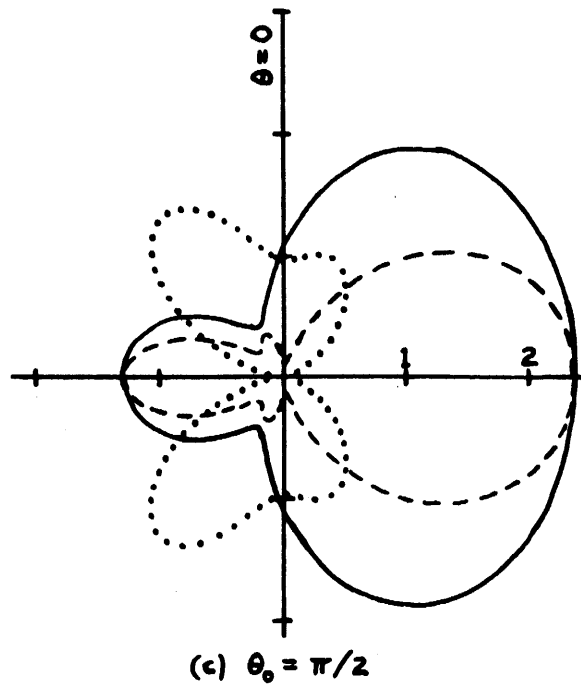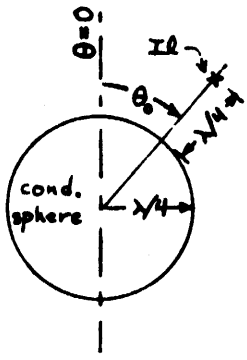
Figure 2. Radiation gain patterns for electric dipoles adjacent to a conducting sphere. Modes m=0,1,2,3 were used in the computer program.
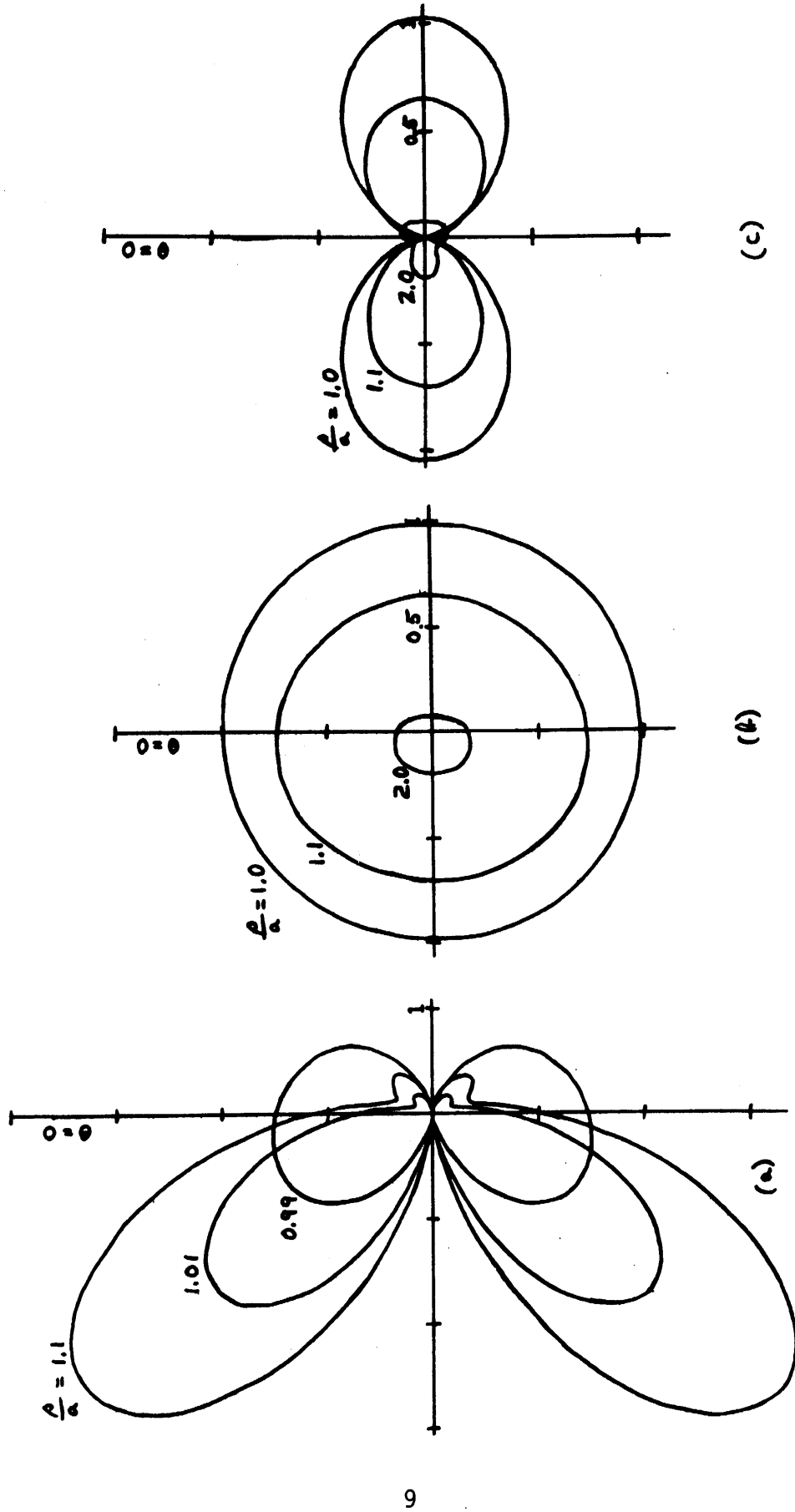
Figure 3. Far-zone $|E^s|^2$ vs. θ for a conducting sphere of radius $a = \lambda/4$ and an electric dipole located at $(r,\theta,\phi) = (\rho,\pi/2,0)$, with ρ varying from outside to inside the sphere. (a) r-directed dipole, (b) ϕ-directed dipole, (c) θ-directed dipole. Modes m=0,1,2,3 were used in the computer program.

about the zero axis. Note that Figures 2 (a), (b), and (c) are related to
each other by a simple rotation in θ, although this fact was not used in
the computations.

A second check was made by using the fact that the scattered field
pattern is the dipole radiation pattern whenever the current element $I\ell$
is inside of S. (This must be so, since $E^i + E^s = 0$ external to S when-
ever $I\ell$ is internal to S.) This check can be applied to bodies of any
shape. The accuracy with which the scattered field approximated the
dipole field was highest when $I\ell$ was near the center of the body, but
remained relatively good even for positions close to the surface. If the
orientation of $I\ell$ is tangential to S, the transition to a dipole field
is smooth as $I\ell$ passes from a point external to a point internal. If the
orientation of $I\ell$ is normal to S, there is an abrupt change in the scat-
tered field as $I\ell$ crosses S. These characteristics are illustrated by
Figure 3 for the case of a conducting sphere. The sphere is of radius
$a = \lambda/4$, and the dipole is located at $\theta = 90°$, $\phi = 0$, ρ variable. Figure
3(a) shows $|E^s|^2$ for a ρ-directed dipole (normal to S) for the positions
$\rho/a = 1.1$, 1.01, 0.99. Note the rapid change to the dipole pattern as
ρ/a changes from 1.01 to 0.99. Figure 3(b) shows $|E^s|^2$ for a ϕ-directed
dipole (tangential to S) for the positions $\rho/a = 2.0$, 1.1, 1.0. Note that
the change to a dipole pattern (perfect circle through 1) is relatively
slow, and is complete when $\rho/a = 1.0$. Figure 3(c) shows $|E^s|^2$ for a z-
directed dipole (tangential to S) for the positions $\rho/a = 2.0$, 1.1, 1.0.
Again the change to a dipole pattern (figure eight through 1) is rela-
tively slow, and is complete when $\rho/a = 1.0$.

As a final check, we can compare the radiation patterns for normal
dipoles on the surface with those for annular slots. The two should be
the same according to the equivalence principle. The patterns for annular
slots can be calculated by the aperture programs of previous reports [2,4].
Figure 4 shows some computations for a cone-sphere. Figure 4(a) compares
the radiation gain pattern if $I\ell$ axially directed and $\lambda/16$ in front of the
tip (position 1) with the radiation pattern of an annular slot (dashed) at
the tip. Figure 4(b) compares the radiation pattern of $I\ell$ axially directed

10
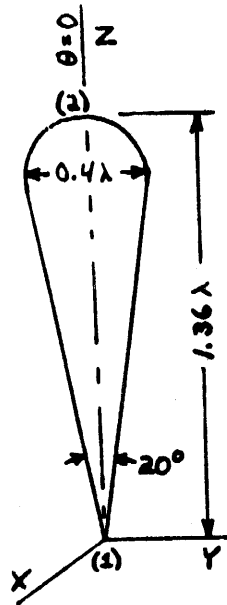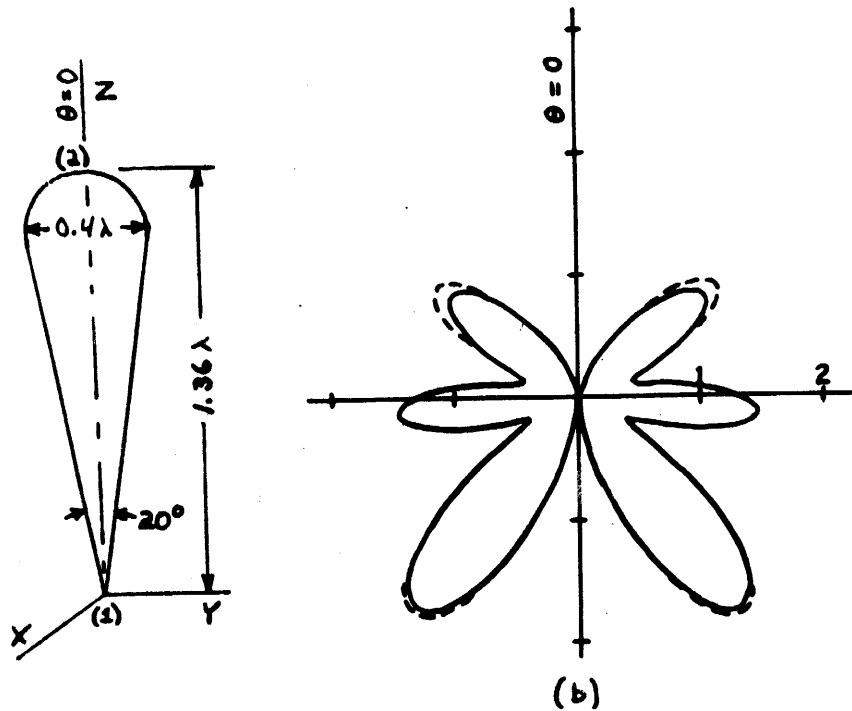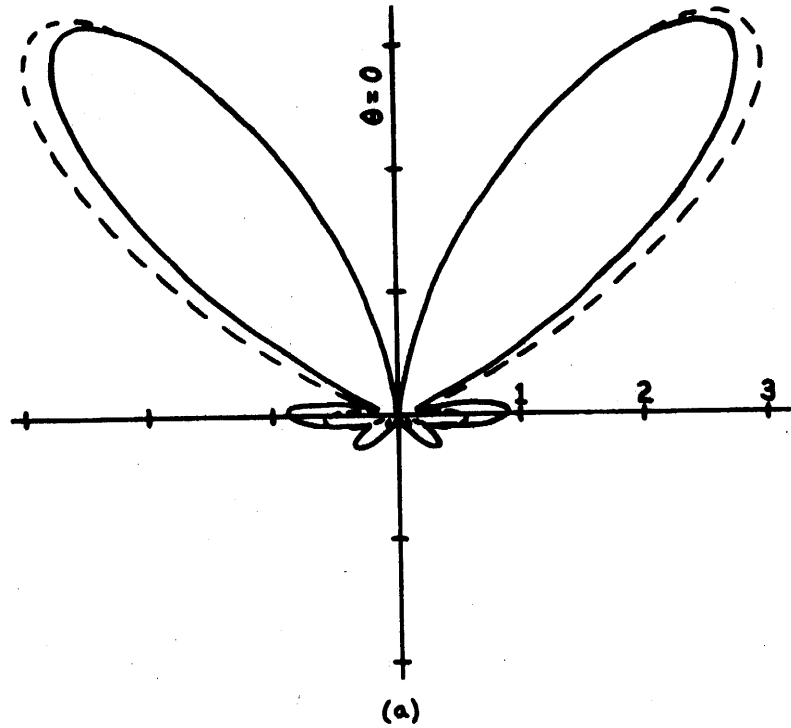
Figure 4. Radiation gain patterns for a cone-sphere excited by an
axially-directed electric dipole (solid) and by an annular
slot (dashed). (a) Dipole λ/16 from, and slot at, cone tip.
(b) Dipole λ/16 from, and slot at, middle of sphere end.

11
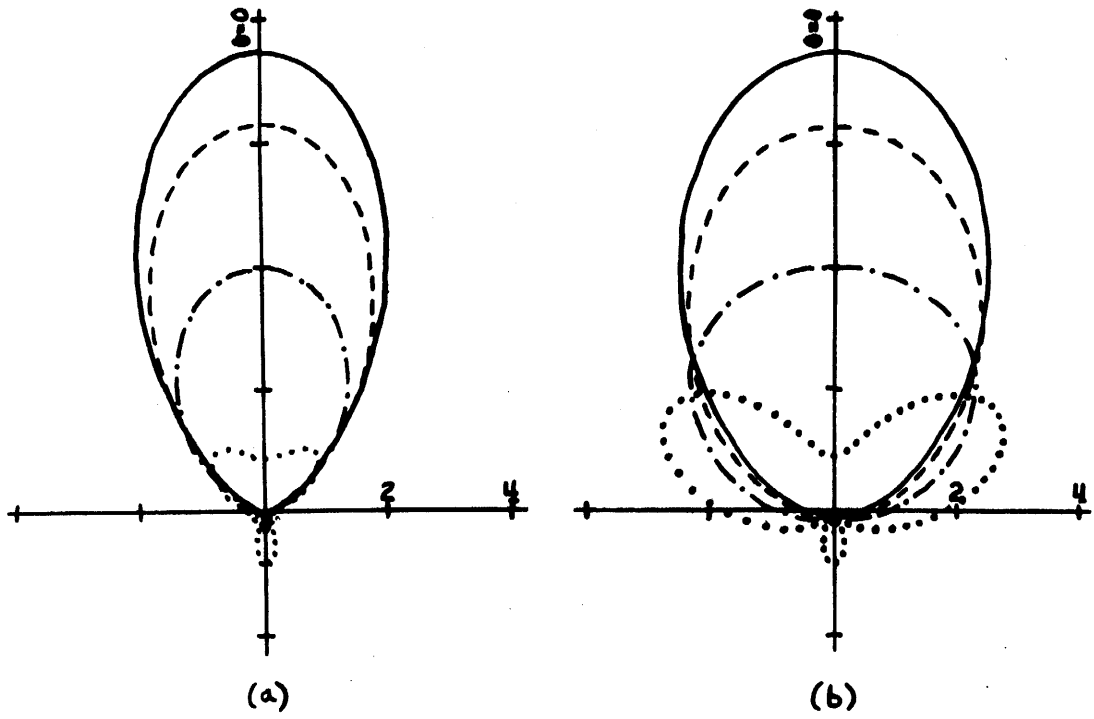
d = λ/8 ————————
d = λ/4 — — — — —
d = 3λ/8 —·—·—·—·—
d = λ/2 ·············
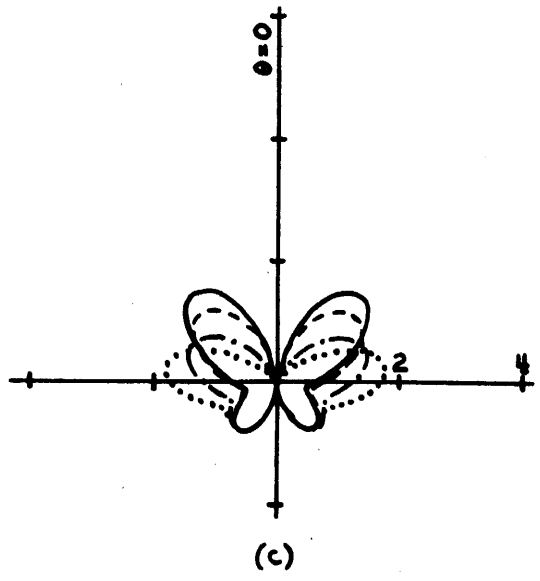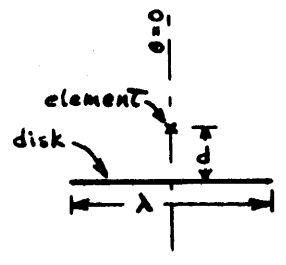
Figure 5. Radiation gain patterns for electric dipoles adjacent
to a conducting disk. (a) x-directed dipoles, (b) y-
directed dipoles, (c) z-directed dipoles.

(a) x-directed Iℓ
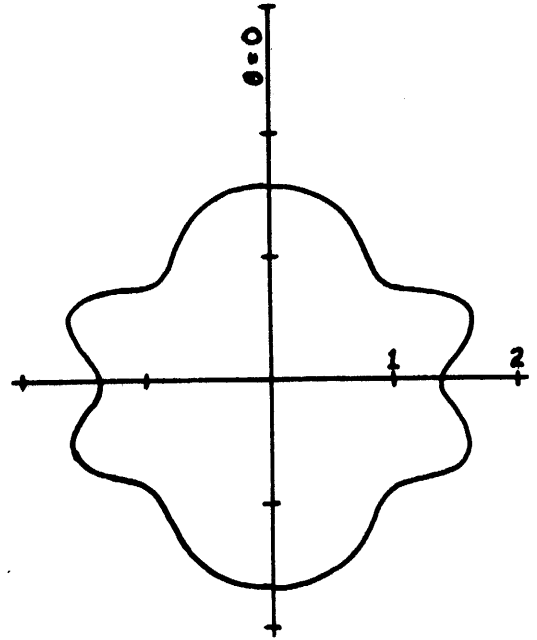
(b) y-directed Iℓ

(c) z-directed Iℓ

Figure 6. Radiation gain patterns for electric dipoles λ/4 from the tip end of a conducting cone-sphere.
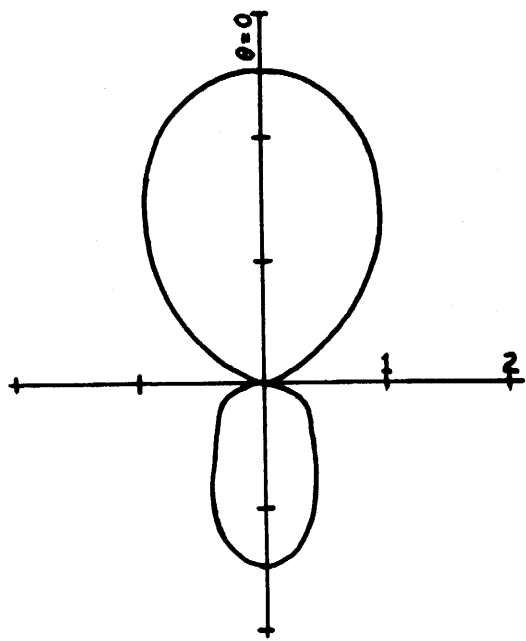
(a) x-directed $I\ell$
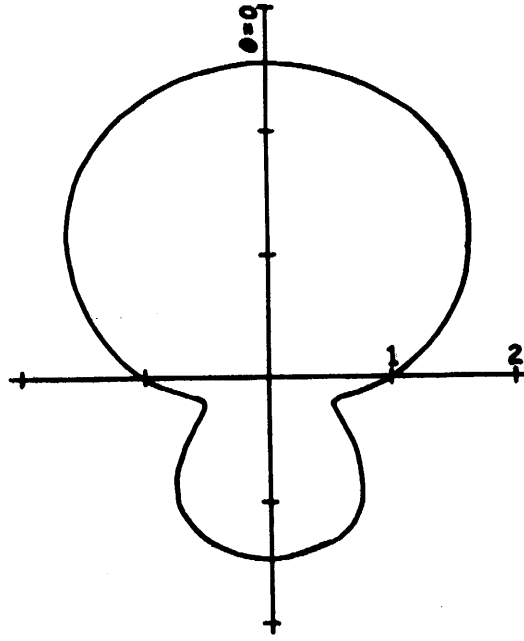
(b) y-directed $I\ell$
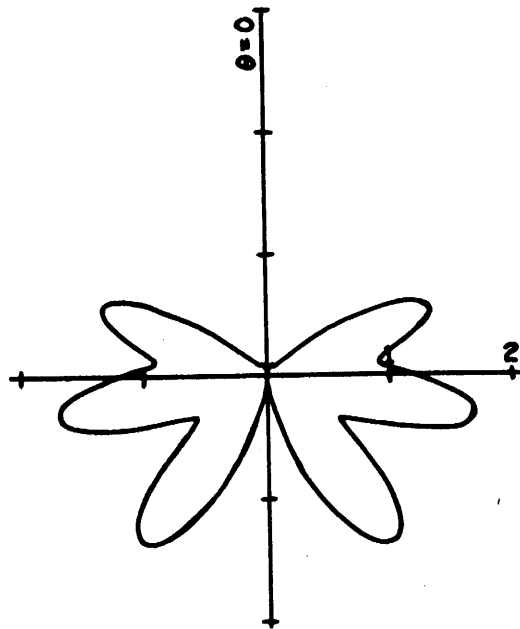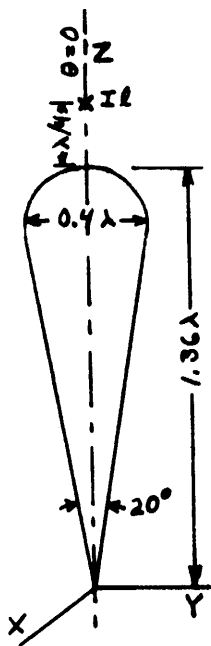
(c) z-directed $I\ell$

Figure 7.   Radiation gain patterns for electric dipoles $\lambda/4$
from the sphere end of a conducting cone-sphere.
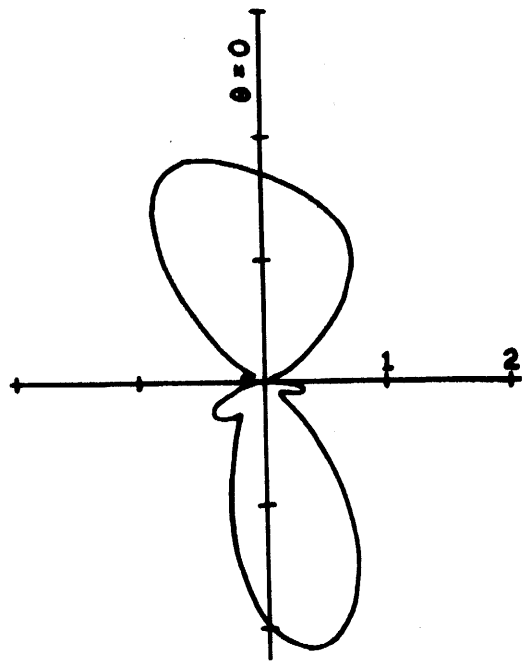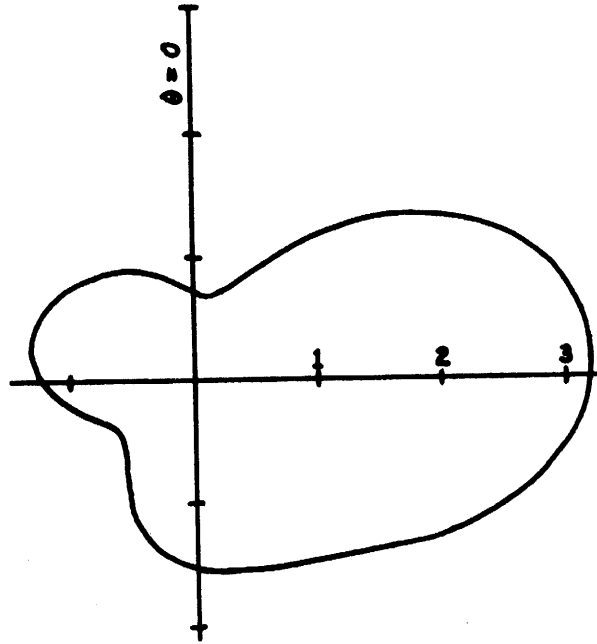
(a) ρ-directed $I\ell$
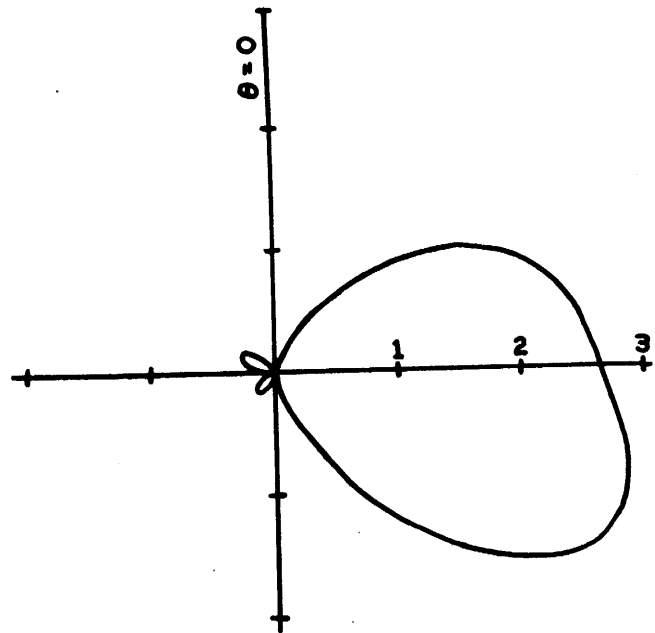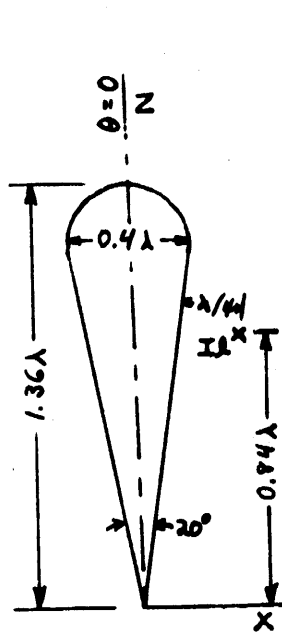
(b) ϕ-directed $I\ell$

(c) z-directed $I\ell$

Figure 8. Radiation gain patterns for electric dipoles $\lambda/4$
from the side of a conducting cone-sphere, about 2/3
way up from tip. Modes m=0,1,2,3 were used in the
computer program.

(a) ρ-directed $I\ell$
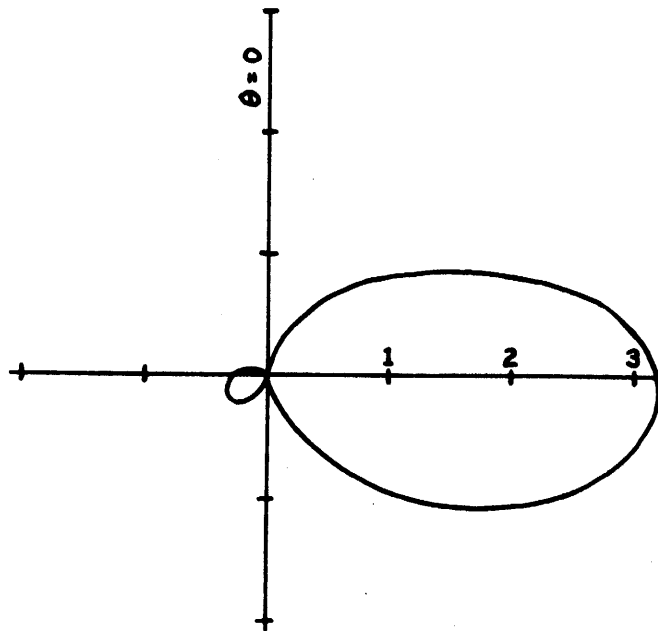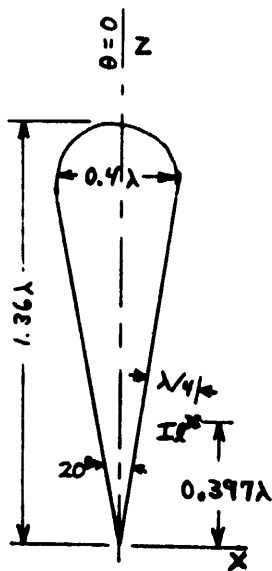
(b) ϕ-directed $I\ell$

(c) z-directed $I\ell$

Figure 9. Radiation gain patterns for electric dipoles $\lambda/4$ from the side of a conducting cone-sphere, about 1/3 way up from tip. Modes m=0,1,2,3 were used in the computer program.

16

and $\lambda/16$ in front of the sphere (position 2) with the radiation pattern of an annular slot (dashed) at the sphere end. The agreement should not be exact in these cases because $I\underset{\sim}{\ell}$ is $\lambda/16$ from S, not exactly on the surface.

Figure 5 shows a typical problem that can be run with the programs of this report. It shows the radiation patterns of dipoles located in front of a conducting disk. This is the finite ground plane problem of interest to many investigators. Figure 5(a) shows the radiation patterns for x-directed dipoles located a distance d = $\lambda/8$, $\lambda/4$, $3\lambda/8$, and $\lambda/2$ in front of the disk. Figure 5(b) shows the radiation patterns for y-directed dipoles at the same positions d. Figures 5(a) and 5(b) correspond to the same physical problem, rotated 90° in space. The patterns of 5(a) are popularly called the E-plane patterns of $I\underset{\sim}{\ell}$, and those of 5(b) the H-plane patterns. Figure 5(c) shows the radiation patterns for z-directed dipoles at the same positions d in front of the disk.

The final sets of patterns, Figures 6 to 9, show radiation gain patterns for dipoles at various positions adjacent to a cone sphere. All patterns are in the $\phi=0$ plane. They are adequately explained by the figure captions, and will not be further discussed here.

IV. DISCUSSION

The computer programs are written explicitly to handle only perfectly conducting bodies, but can be easily modified to handle loaded bodies according to the concepts of Section II. Imperfectly conducting bodies, and bodies thinly coated by dielectric or magnetic materials, can be treated by considering the body to be continuously loaded with the proper surface impedance. A detailed treatment of loaded bodies with computer programs is given in Report No. 4 [2].

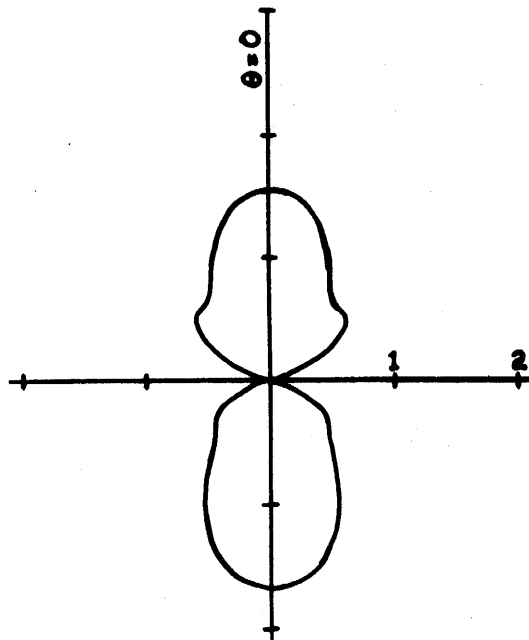The general program of this report apparently gives good accuracy for far-field quantities so long as the number of current expansion functions is about ten per wavelength of the contour. Near-field quantities, such as current on the body, are less accurate. Accuracy also depends on such things

as body shape and closeness of the current element to the body. For example, if $I\underset{\sim}{\ell}$ is very near the surface the current becomes nearly singular. Better accuracy for specific problems can be obtained by mathematically introducing the proper singularity, but this cannot be done for a general program.

As emphasized earlier, the programs of this report are valid for both external and internal problems. They should therefore be useful for the design of resonant cavities with feed systems, as well as for external antenna and scatterer problems. The principal limitation to the usefulness of the solution is that imposed by matrix inversion. To keep computer time and storage within reasonable bounds, we are limited to bodies whose generating contours are a few wavelengths long.

V. DETAILS OF THE SOLUTION

This section gives the details of the moment solution evaluated for perfectly conducting bodies of revolution. The notation is that used in previous reports [2,4,6]. The coordinates are as defined in Figure 1; a point in space is specified in terms of cylindrical coordinates (ρ, ϕ, z), and a point on S in terms of surface coordinates (t, ϕ).

If a perfectly conducting body of revolution is immersed in an incident electric field $\underset{\sim}{E}^i$, the induced electric current $\underset{\sim}{J}$ on the surface S of the body can be approximated by

$$\underset{\sim}{J} = \sum_{m=-M}^{M} \sum_{i=1}^{N} (I_{mi}^t \underset{\sim}{J}_{mi}^t + I_{mi}^\phi \underset{\sim}{J}_{mi}^\phi) \tag{15}$$

where I_{mi}^t and I_{mi}^ϕ are constants to be determined and $\underset{\sim}{J}_{mi}^t$ and $\underset{\sim}{J}_{mi}^\phi$ are expansion functions of the type

$$\underset{\sim}{J}_{mi}^t = \underset{\sim}{u}_t \, f_i(t) e^{jm\phi}$$

$$\tag{16}$$

$$\underset{\sim}{J}_{mi}^\phi = \underset{\sim}{u}_\phi \, f_i(t) e^{jm\phi}$$

Here $\underset{\sim}{u}_t$ and $\underset{\sim}{u}_\phi$ are the unit vectors of the orthogonal coordinate system (t, ϕ) on S and $f_i(t)$ is a real triangular function divided by the distance ρ from the axis of the body of revolution. The constants I_{mi}^t and I_{mi}^ϕ are obtained from

$$\begin{bmatrix} [I_m^t] \\ \\ [I_m^\phi] \end{bmatrix} = \begin{bmatrix} [Y_m^{tt}] & [Y_m^{t\phi}] \\ \\ [Y_m^{\phi t}] & [Y_m^{\phi\phi}] \end{bmatrix} \begin{bmatrix} [V_m^t] \\ \\ [V_m^\phi] \end{bmatrix} \tag{17}$$

where

$$[I_m^t] = [I_{m1}^t \ I_{m2}^t \ \cdots \ I_{mN}^t]$$
$$\tag{18}$$
$$[I_m^\phi] = [I_{m1}^\phi \ I_{m2}^\phi \ \cdots \ I_{mN}^\phi]$$

$$[V_m^t] = [V_{m1}^t \ V_{m2}^t \ \cdots \ V_{mN}^t]$$
$$\tag{19}$$
$$[V_m^\phi] = [V_{m1}^\phi \ V_{m2}^\phi \ \cdots \ V_{mN}^\phi]$$

$$V_{mi}^t = \iint_S \underset{\sim}{E}^i \cdot \underset{\sim}{W}_{mi}^t \ ds$$
$$\tag{20}$$
$$V_{mi}^\phi = \iint_S \underset{\sim}{E}^i \cdot \underset{\sim}{W}_{mi}^\phi \ ds$$

$$\underset{\sim}{W}_{mi}^t = \underset{\sim}{u}_t \ f_i(t) e^{-jm\phi}$$
$$\tag{21}$$
$$\underset{\sim}{W}_{mi}^\phi = \underset{\sim}{u}_\phi \ f_i(t) e^{-jm\phi}$$

The Y matrix of (17) is the generalized admittance matrix for the body of revolution. The V matrix of (17) is the generalized voltage matrix for the excitation.

The matrix elements V_{mi}^t and V_{mi}^ϕ will be obtained for a current element $I\ell$ located at $\phi=0$ either inside or outside the surface S of the body of revolution. Equation (20) may be integrated by parts to obtain

$$V_{mi} = - j\omega \iint_S (\underset{\sim}{A} \cdot \underset{\sim}{W}_{mi} + \Phi\sigma_i)ds \qquad (22)$$

where V_{mi} and $\underset{\sim}{W}_{mi}$ are either V_{mi}^t and $\underset{\sim}{W}_{mi}^t$ or V_{mi}^ϕ and $\underset{\sim}{W}_{mi}^\phi$. $\underset{\sim}{A}$ and Φ are respectively the magnetic vector potential and electric scalar potential associated with the electric field $\underset{\sim}{E}^1$ of the dipole $I\underset{\sim}{\ell}$. Also, σ_i is the electric charge associated with $\underset{\sim}{W}_{mi}$. The potentials $\underset{\sim}{A}$ and ϕ are given by

$$\underset{\sim}{A} = \frac{-jk\mu}{4\pi} I\underset{\sim}{\ell} \; h_o^{(2)}(k|\underset{\sim}{r}-\underset{\sim}{r}'|)$$

$$\qquad (23)$$

$$\Phi = \frac{\eta}{4\pi} I\underset{\sim}{\ell} \cdot \underset{\sim}{\nabla} h_o^{(2)}(k|\underset{\sim}{r}-\underset{\sim}{r}'|)$$

where $h_o^{(2)}(x) = \dfrac{e^{-jx}}{-jx}$ is a spherical Bessel function of the third kind and $|\underset{\sim}{r}-\underset{\sim}{r}'|$ is the distance from the dipole at $\underset{\sim}{r}'$ to a point $\underset{\sim}{r}$ on S. The gradient operation $\underset{\sim}{\nabla}$ is with respect to unprimed coordinates. The current function $\underset{\sim}{W}_{mi}$ may be either

$$\underset{\sim}{W}_{mi}^t = \underset{\sim}{u}_t \; f_i(t)e^{-jm\phi}$$

$$\qquad (24)$$

$$\sigma_i^t = \frac{-1}{j\omega\rho} \frac{d}{dt} (\rho f_i)e^{-jm\phi}$$

or

$$\underset{\sim}{W}_{mi}^\phi = \underset{\sim}{u}_\phi \; f_i(t)e^{-jm\phi}$$

$$\qquad (25)$$

$$\sigma_i^\phi = \frac{m}{\omega\rho} f_i(t)e^{-jm\phi}$$

Equations (23), (24) and (25) are introduced into equation (22).

$$V_{mi}^{t} = \frac{\eta}{4\pi} \left[-k^2 \int dt \; \rho f_1(t) \int d\phi \; (I\underset{\sim}{\ell} \cdot \underset{\sim}{u}_t) \; h_o^{(2)} \; e^{-jm\phi} \right.$$

$$\left. + \int dt \; \frac{d}{dt} (\rho f_1) \int d\phi \; (I\underset{\sim}{\ell} \cdot \underset{\sim}{\nabla} h_o^{(2)}) \; e^{-jm\phi} \right] \tag{26}$$

$$V_{mi}^{\phi} = \frac{\eta}{4\pi} \left[-k^2 \int dt \; \rho f_1(t) \int d\phi \; (I\underset{\sim}{\ell} \cdot \underset{\sim}{u}_\phi) \; h_o^{(2)} \; e^{-jm\phi} \right.$$

$$\left. -jm \int dt \; f_1(t) \int d\phi \; (I\underset{\sim}{\ell} \cdot \underset{\sim}{\nabla} h_o^{(2)}) \; e^{-jm\phi} \right] \tag{27}$$

Equations (26) and (27) may be integrated numerically in both ϕ and t, but spherical wave functions are introduced instead. If the spherical Bessel function and Legendre polynomials are expanded [5],

$$h_o^{(2)}(k|\underset{\sim}{r}-\underset{\sim}{r}'|) = \sum_{-\infty}^{\infty} G_m \; e^{jm\phi} \tag{28}$$

where

$$G_m = G_{-m} = \begin{cases} \displaystyle\sum_{n=m}^{\infty} \frac{(2n+1)(n-m)!}{(n+m)!} \; h_n^{(2)}(kr') \; j_n(kr) \; P_n^m(\cos\theta) \; P_n^m(\cos\theta') & r'>r \\[2em] \displaystyle\sum_{n=m}^{\infty} \frac{(2n+1)(n-m)!}{(n+m)!} \; h_n^{(2)}(kr) \; j_n(kr') \; P_n^m(\cos\theta) \; P_n^m(\cos\theta') & r'<r \end{cases} \tag{29}$$

In (29), $m=0,1,2,\ldots$. The angle ϕ' does not appear in (28) because the dipole is located such that $\phi' = 0$. For the ϕ integrations in (26) and (27), an origin (fixed with respect to ϕ but variable with respect to t) is chosen on the axis of the body of revolution so that $\underset{\sim}{r} \cdot \underset{\sim}{u}_z = 0$. If $I\underset{\sim}{\ell}$ has x, y, and z components,

$$\underset{\sim}{u}_t = \underset{\sim}{u}_x \sin v \cos \phi + \underset{\sim}{u}_y \sin v \sin \phi + \underset{\sim}{u}_z \cos v$$

is needed for the $I\underset{\sim}{\ell} \cdot \underset{\sim}{u}_t$ term in (26). For the $I\underset{\sim}{\ell} \cdot \underset{\sim}{u}_\phi$ term in (27)

$$\underset{\sim}{u}_\phi = - \underset{\sim}{u}_x \sin \phi + \underset{\sim}{u}_y \cos \phi.$$

For the $I\underset{\sim}{\ell} \cdot \underset{\sim}{\nabla} h_o^{(2)}$ term in (26) and (27), $I\underset{\sim}{\ell}$ can be expressed in terms of the unit vectors $\underset{\sim}{u}_r$, $\underset{\sim}{u}_\theta$ and $\underset{\sim}{u}_\phi$ instead of $\underset{\sim}{u}_x$, $\underset{\sim}{u}_y$ and $\underset{\sim}{u}_z$.

$$\underset{\sim}{u}_x = \underset{\sim}{u}_r \cos \phi - \underset{\sim}{u}_\phi \sin \phi$$

$$\underset{\sim}{u}_y = \underset{\sim}{u}_r \sin \phi + \underset{\sim}{u}_\phi \cos \phi$$

$$\underset{\sim}{u}_z = - \underset{\sim}{u}_\theta$$

An x-directed dipole $\underset{\sim}{u}_x I\ell_x$ leads to

$$V_{mi}^t = \frac{\eta I\ell_x}{2} \left[-k^2 \int dt \, \rho f_i(t) \sin v \, \frac{G_{m+1} + G_{m-1}}{2} \right.$$

$$(30)$$

$$\left. + \int dt \, \frac{d}{dt} (\rho f_i) \left(\frac{\frac{\partial G_{m+1}}{\partial r} + \frac{\partial G_{m-1}}{\partial r}}{2} + \frac{(m+1)G_{m+1} - (m-1)G_{m-1}}{2\rho} \right) \right]$$

$$V_{mi}^\phi = \frac{\eta I\ell_x}{2} \left[-k^2 \int dt \, \rho f_i(t) \, \frac{G_{m+1} - G_{m-1}}{2j} \right.$$

$$\left. -jm \int dt \, f_i(t) \left(\frac{\frac{\partial G_{m+1}}{\partial r} + \frac{\partial G_{m-1}}{\partial r}}{2} + \frac{(m+1)G_{m+1} - (m-1)G_{m-1}}{2\rho} \right) \right]$$

A y-directed dipole $\underset{\sim}{u}_y I\ell_y$ leads to

$$V_{mi}^t = \frac{\eta I \ell_y}{2} \left[-jk^2 \int dt\, \rho f_1(t) \sin v\, \frac{G_{m+1} - G_{m-1}}{2} \right.$$

$$\left. + j \int dt\, \frac{d}{dt}(\rho f_1) \left(\frac{\frac{\partial G_{m+1}}{\partial r} - \frac{\partial G_{m-1}}{\partial r}}{2} + \frac{(m+1)G_{m+1} + (m-1)G_{m-1}}{2\rho} \right) \right] \tag{31}$$

$$V_{mi}^\phi = \frac{\eta I \ell_y}{2} \left[-k^2 \int dt\, \rho f_1(t)\, \frac{G_{m+1} + G_{m-1}}{2} \right.$$

$$\left. + m \int dt\, f_1(t) \left(\frac{\frac{\partial G_{m+1}}{\partial r} - \frac{\partial G_{m-1}}{\partial r}}{2} + \frac{(m+1)G_{m+1} + (m-1)G_{m-1}}{2\rho} \right) \right]$$

A z-directed dipole $\underset{\sim}{u}_z\, I\ell_z$ yields

$$V_{mi}^t = \frac{\eta I \ell_z}{2} \left[-k^2 \int dt\, \rho f_1(t) \cos v\, G_m - \int dt\, \frac{d}{dt}(\rho f_1)\, \frac{1}{\rho} \frac{\partial G_m}{\partial \theta} \right] \tag{32}$$

$$V_{mi}^\phi = \frac{\eta I \ell_z}{2}\, (jm) \int dt\, f_1(t)\, \frac{1}{\rho} \frac{\partial G_m}{\partial \theta}$$

Because the origin is at $\underset{\sim}{r} \cdot \underset{\sim}{u}_z = 0$ on the axis of the body of revolution, (29) becomes

$$G_m = G_{-m} = \begin{cases} \displaystyle\sum_{n=m}^{\infty} \frac{(2n+1)(n-m)!}{(n+m)!}\, h_n^{(2)}(kr')\, j_n(k\rho)\, P_n^m(0)\, P_n^m(\cos \theta') & r' > \rho \\[4ex] \displaystyle\sum_{n=m}^{\infty} \frac{(2n+1)(n-m)!}{(n+m)!}\, h_n^{(2)}(k\rho) j_n(kr')\, P_n^m(0)\, P_n^m(\cos \theta') & r' < \rho \end{cases}$$

23

where $m = 0, 1, 2 \ldots$. The quantities $\frac{\partial G_m}{\partial r}$ and $\frac{\partial G_m}{\partial \theta}$ are obtained by differentiating (29) term by term then setting $r = \rho$ and $\cos \theta = 0$. If the dipole $I\underset{\sim}{\ell}$ is rotated from its original position at $\phi' = 0$ to $\phi' \neq 0$, expressions (30) to (32) must be multiplied by $e^{-jm\phi'}$.

The current $\underset{\sim}{J}$ induced on S by the dipole $I\underset{\sim}{\ell}$ located at $\phi' = 0$ gives rise to a scattered electric field $\underset{\sim}{E}^S$. The scattered electric field in the direction of a receiving dipole $I\underset{\sim}{\ell}_r$ is given by

$$\underset{\sim}{E}^S \cdot I\underset{\sim}{\ell}_r = \sum_{m=-M}^{M} [\widetilde{V}_{-m}]^r [Y_m][V_m]^t e^{jm\phi} \qquad (34)$$

where $[V_m]^t$ is the matrix $\begin{bmatrix} [V_m^t] \\ [V_m^\phi] \end{bmatrix}$ calculated using the incident electric

field of the transmitting dipole $I\underset{\sim}{\ell}$. The $[V_m]^r e^{-jm\phi}$ is $\begin{bmatrix} [V_m^t] \\ [V_m^\phi] \end{bmatrix}$ calculated

using the field of the receiving dipole $I\underset{\sim}{\ell}_r$. Notice that $[V_m]^r$ is the generalized voltage matrix that would result if $I\underset{\sim}{\ell}_r$ were located at $\phi = 0$. Because

1) $[Y_m^{tt}]$ and $[Y_m^{\phi\phi}]$ are even in m

2) $[Y_m^{t\phi}]$ and $[Y_m^{\phi t}]$ are odd in m

3) V_{mi}^t of (30) and (32) are even in m

4) V_{mi}^ϕ of (30) and (32) are odd in m

5) V_{mi}^t of (31) is odd in m

6) V_{mi}^ϕ of (31) is even in m,

the +m and −m terms appearing in (15) and (34) may be combined if the directions of $I\underset{\sim}{\ell}$ and $I\underset{\sim}{\ell}_r$ are restricted. Recall that $I\underset{\sim}{\ell}$ is located in the $\phi' = 0$ plane. Define four different polarizations

24

1) $I\underset{\sim}{\ell} \cdot u_{\sim\phi} = 0$ and $I\underset{\sim}{\ell}_r \cdot u_{\sim\phi} = 0$

2) $I\underset{\sim}{\ell} \cdot u_{\sim\phi} = 0$ and $I\underset{\sim}{\ell}_r \cdot u_{\sim\rho} = I\underset{\sim}{\ell}_r \cdot u_{\sim z} = 0$

3) $I\underset{\sim}{\ell} \cdot u_{\sim\rho} = I\underset{\sim}{\ell} \cdot u_{\sim z} = 0$ and $I\underset{\sim}{\ell}_r \cdot u_{\sim\phi} = 0$

4) $I\underset{\sim}{\ell} \cdot u_{\sim\rho} = I\underset{\sim}{\ell} \cdot u_{\sim z} = 0$ and $I\underset{\sim}{\ell}_r \cdot u_{\sim\rho} = I\underset{\sim}{\ell}_r \cdot u_{\sim z} = 0$

For polarizations #1 and #2

$$\underset{\sim}{J} = \sum_{m=0}^{M} [\widetilde{f}(t)][I_m^t]\underset{\sim}{u}_t \epsilon_m \cos m\phi + \sum_{m=1}^{M} [\widetilde{f}(t)][I_m^\phi] \underset{\sim}{u}_\phi\, 2j \sin m\phi \tag{35}$$

where

$$[\widetilde{f}(t)] = [f_1(t) \ldots f_N(t)] \tag{36}$$

and

$$\epsilon_m = \begin{cases} 1 & m=0 \\ 2 & m>0 \end{cases} \tag{37}$$

For polarizations #3 and #4,

$$\underset{\sim}{J} = \sum_{m=1}^{M} [\widetilde{f}(t)][I_m^t]\, \underset{\sim}{u}_t\, 2j \sin m\phi + \sum_{m=0}^{M} [\widetilde{f}(t)][I_m^\phi]\, \underset{\sim}{u}_\phi \epsilon_m \cos m\phi \tag{38}$$

For polarizations #1 and #4

$$\underset{\sim}{E}^s \cdot I\underset{\sim}{\ell}_r = \sum_{m=0}^{M} [\widetilde{V}_{-m}]^r [Y_m][V_m]^t \epsilon_m \cos m\phi \tag{39}$$

For polarizations #2 and #3

$$\underset{\sim}{E}^s \cdot I\underset{\sim}{\ell}_r = \sum_{m=1}^{M} [V_{-m}]^r [Y_m][V_m]^t\, 2j \sin m\phi \tag{40}$$

The $[V_m]^r$ in (39) and (40) are calculated from the electric field which would result if $I\underset{\sim}{\ell}_r$ were located at $\phi=0$. Arbitrarily directed dipoles $I\underset{\sim}{\ell}$ and $I\underset{\sim}{\ell}_r$ may be obtained as a superposition of the four polarizations. Location of $I\underset{\sim}{\ell}$ in the $\phi'=0$ plane is not a severe restriction because $\underset{\sim}{J}$ and $\underset{\sim}{E}^s$ for $I\underset{\sim}{\ell}$ at $\phi'=\phi_0$ can be obtained by rotating $\underset{\sim}{J}$ and $\underset{\sim}{E}^s$ for $I\underset{\sim}{\ell}$ at $\phi'=0$ through an angle ϕ_0.

25

For distant dipoles $I\underset{\sim}{\ell}_r$, equation (34) becomes

$$\underset{\sim}{E}^s \cdot \underset{\sim}{u}_\theta = \frac{-j\omega\mu e^{-jkr}}{4\pi r} \sum_{m=-M}^{M} [R_m]^\theta [Y_m][V_m]^t e^{jm\phi}$$

(41)

$$\underset{\sim}{E}^s \cdot \underset{\sim}{u}_\phi = \frac{-j\omega\mu e^{-jkr}}{4\pi r} \sum_{m=-M}^{M} [R_m]^\phi [Y_m][V_m]^t e^{jm\phi}$$

where

$$[R_m]^\theta = [R_m^{t\theta}] \, [R_m^{\phi\theta}]$$

(42)

$$[R_m]^\phi = [R_m^{t\phi}] \, [R_m^{\phi\phi}]$$

in which $[R_m^{t\theta}]$, $[R_m^{\phi\theta}]$, $[R_m^{t\phi}]$, and $[R_m^{\phi\phi}]$ are row matrices whose elements are given by equations (77) and (81) of a previous report [6]. The $+m$ and $-m$ terms appearing in (41) may be combined in the same manner as those appearing in (34).

The gains G_θ and G_ϕ of a far field pattern $\underset{\sim}{E}$ are given by

$$G_\theta = \frac{4\pi r^2 |\underset{\sim}{E} \cdot \underset{\sim}{u}_\theta|^2}{\eta P}$$

(43)

$$G_\phi = \frac{4\pi r^2 |\underset{\sim}{E} \cdot \underset{\sim}{u}_\phi|^2}{\eta P}$$

where $\underset{\sim}{E} \cdot \underset{\sim}{u}_\theta$ and $\underset{\sim}{E} \cdot \underset{\sim}{u}_\phi$ are evaluated in the far zone and P is the total power radiated. The total electric field $\underset{\sim}{E}$ of a dipole $I\underset{\sim}{\ell}$ radiating near a perfectly conducting body of revolution is a superposition of the dipole field $\underset{\sim}{E}^d$ and the field $\underset{\sim}{E}^s$ of the current induced on the surface of the body of revolution.

$$\underset{\sim}{E} = \underset{\sim}{E}^s + \underset{\sim}{E}^d$$

(44)

The far field of a dipole located at $\underset{\sim}{r}'$ is given by

26

$$\underset{\sim}{E}^d \cdot \underset{\sim}{u}_\theta = \frac{-j\omega\mu e^{-jkr}}{4\pi r} \; e^{jkr'\cos\alpha} \underset{\sim}{I\ell} \cdot \underset{\sim}{u}_\theta$$

(45)

$$\underset{\sim}{E}^d \cdot \underset{\sim}{u}_\phi = \frac{-j\omega\mu e^{-jkr}}{4\pi r} \; e^{jkr'\cos\alpha} \underset{\sim}{I\ell} \cdot \underset{\sim}{u}_\theta$$

where α is the angle between $\underset{\sim}{r}$ and $\underset{\sim}{r}'$.

If there are no losses, the power P radiated is equal to the power required to maintain the electric current sources of $\underset{\sim}{E}$. This power P is given by

$$P = - \text{Real} \int \underset{\sim}{E}^d \cdot d(\underset{\sim}{I\ell})^* + \left|I\ell\right|^2 \text{Real} \left[\frac{-\underset{\sim}{E}^s \cdot (\underset{\sim}{I\ell})^*}{\left|I\ell\right|^2} \right]$$

(46)

In (46), the term $-\text{Real} \int \underset{\sim}{E}^d \cdot d(\underset{\sim}{I\ell})^*$ is recognized as the power of the isolated dipole $\underset{\sim}{I\ell}$ which can be more conveniently calculated by integrating the field pattern (45). The complex number $\dfrac{-\underset{\sim}{E}^s \cdot (\underset{\sim}{I\ell}^*)}{\left|I\ell\right|^2}$

is defined as the "mutual impedance" Z_{mut} between the dipole and the body of revolution. Z_{mut} is obtained by setting $\underset{\sim}{I\ell}_r = \underset{\sim}{I\ell}$ in (34).

$$P = \left|I\ell\right|^2 \left(\frac{\eta k^2}{6\pi} + \text{Real } Z_{\text{mut}}\right)$$

(47)

VI. PROGRAM INSTRUCTIONS

The first computer program calculates the generalized voltage matrices whose elements are given by (30), (31) and (32). Punched card data is read early in the main program according to

```
50   READ(1,51,END=52) KV,NP,BK
51   FORMAT(2I3,E14.7)
     READ(1,53)(RH(I),I=1,NP)
     READ(1,53)(ZH(I),I=1,NP)
53   FORMAT(10F8.4)
```

A voltage matrix is calculated for each of KV dipoles. RH(I) and ZH(I) are respectively the distance ρ from the axis of the body of revolution and the z coordinate measured along the axis for the Ith data point on the generating curve of the body of revolution. There should be a data point at both extremities of the generating curve. NP must be odd. BK is the propagation constant $k = \omega\sqrt{\mu\epsilon}$. More punched card data is read later in the main program according to

```
         DO 200 K=1,KV
         K1 = K+1
         READ(1,201) M1(K1),N1(K1),XR(K1),XP(K1),XZ(K1),
                     UR(K1),UP(K1),UZ(K1)
  201    FORMAT(2I3,6F9.4)
  200    CONTINUE
```

The index K indicates the Kth dipole. For the moment, M1(1),N1(1),...UZ(1) are left undefined. The voltage matrix $[V_m]^t$ appearing in (34) will be calculated for m = M1. The infinite series (33) is truncated such that $m \leq n \leq$ N1. The dipole $\underset{\sim}{I\ell}$ is located at $(\rho,\phi,z) =$ (XR,XP,XZ). XP is in degrees. The ρ,ϕ and z components of $\underset{\sim}{I\ell}$ are given by

$$\underset{\sim}{I\ell} = UR\underset{\sim}{u}_\rho + UP\underset{\sim}{u}_\phi + UZ\underset{\sim}{u}_z$$

If several dipoles have the same XR and XZ, it is more efficient to group them together, putting a dipole which has simultaneously the largest M1 and N1 first. In this way the spherical Bessel functions and associated Legendre polynomials need to be computed only once for the whole group. If several dipoles have the same M1 and N1 as well as the same XR and XZ, it is more efficient to group them together. The program calculates (30), (31), and (32) and stores them when it encounters the first dipole. All the dipoles in the group are then obtained by weighting (30), (31), and (32) by UR, UP, and UZ. The coordinate XP is obtained by multiplying the net result by $e^{-j(M1)\cdot(XP)}$.

The sample data for the first program is that for one dipole outside a cone-sphere of total cone angle 20° and sphere radius 0.2 wavelength. The

sphere and cone surfaces are tangent to each other at the cone to sphere junction. The data RH and ZH were computed by a short auxiliary computer program not listed here. The total length of the generating curve is arbitrarily taken to be 20 meters. The data points are taken every half meter along the generating curve. The dipole is located in the $\phi=0$ plane 0.25 wavelength from the 13th data point

$$RH = 1.0419$$

$$ZH = 5.9088$$

The 0.25 wavelength is measured in the $\phi=0$ plane perpendicular to the cone surface. The dipole is of unit amplitude in the ρ direction.

$$I\underset{\sim}{\ell} = \underset{\sim}{u}_\rho$$

At the end of the program, the voltage is printed according to

      WRITE(3,228)(V(J),J=1,NM2)

228   FORMAT(1X,10G11.4)

and punched according to

      WRITE(2,241)(V(J),J=1,NM2)

241   FORMAT(7E11.4)

Here, $\dfrac{NM2}{2}$ corresponds to the N of equation (19) and

$$V^t_{m1}, \ V^t_{m2}, \ \cdots \ V_{m\frac{NM2}{2}}, \ V^\phi_{m1}, \ V^\phi_{m2}, \ \cdots \ V^\phi_{m\frac{NM2}{2}}$$

reside in that order in the complex variable V.

If the first and last data points on the generating curve of the body of revolution are the same, the six statements following statement 126 set KL=0 and overlap the second and third data points. If the first and last data points are different, KL remains at one. In Do loop 57 where I2=I-1, DH(I2) is the distance between the I2[th] and I[th] data points on the generating curve. Do loop 57 also calculates R(I2), ZS(I2), SV(I2) and CV(I2) respectively ρ, z, sin v and cos v midway between the I2[th] and I[th] data points on the generating curve. Here, v is the angle between $\underset{\sim}{u}_t$ and the z axis.

In Do loop 74, $T(4*(J-1)+I)$, $I=1,2,3,4$ is the $\rho f_J(t)$ appearing in (30) sampled midway between the $[2\times(J-1)+I]^{th}$ and $[2\times(J-1)+I+1]^{th}$ data points on the generating curve and multiplied by $DH(2\times(J-1)+I)$. TP represents $\frac{d}{dt}(\rho f_J(t))$ times DH. If KL=0, TR is the same as T. The T represents $f_i(t)$ associated with $\underset{\sim mi}{J^t}$ in (16) and the TR represents $f_i(t)$ associated with $\underset{\sim mi}{J^\phi}$. If KL=1 and $RH(1) \neq 0$, the logic between statements 77 and 23 changes $\rho f_1(t)$ from a triangular function to a piecewise linear function which is 2 at the first data point, 1 at the third and 0 at the fifth. Similarly, the logic between statements 79 and 78 modifies the last function $\rho f_{NM}(t)$. Do loop 231 puts n! in PS(n+1).

In Do loop 200, K refers to the Kth dipole. In statement 246, the complex number U4 is $\frac{n}{4}e^{-jm\phi}$. If M1, N1, XR and XZ are unchanged from the previous dipole, execution proceeds to statement 235 where Do loop 237 calculates V from the previously computed V1, V2, and V3. If at least one of the variables M1, N1, XR and XZ is different from that of the previous dipole, execution proceeds to statement 236. The spherical Bessel functions and their derivatives of argument kr and order 0,1,2,...N2-1 have been previously calculated. If N1 is larger than N2-1, the spherical Bessel functions and their derivatives are calculated by the subroutine BES in Do loop 208. The subroutine BES(L,LD,ID,NJ,XJ,BJ,BJP,BY,BYP) puts $j_n(XJ)$, n=0,1,2,...(NJ-1) in BJ(L1+1) through BJ(L1+NJ) and $y_n(XJ)$, n=0,1,2...(NJ-1) in BY(L1+1) through BY(L1+NJ). If ID is not 2, $j_n'(XJ)$, is put in BJP(L3+1) through BJP(L3+NJ) and $y_n'(XJ)$ in BYP(L3+1) through BYP(L3+NJ). As in BES, L1 = (L-1)*NJ and L3 = (LD-1)*NJ. The associated Legendre polynomials $P_n^m(\cos\theta)$ and their derivatives $\frac{d}{d\theta}P_n^m(\cos\theta)$ have been previously calculated for m=0,1,2,...M2-1 and n=m,m+1,...N2-1. If either N1 > N2-1 or M1 > M2-2 or both, $P_n^m(\cos\theta)$ and $\frac{d}{d\theta}P_n^m(\cos\theta)$ are calculated by statement 244. The subroutine LEG(L,LD,ID,NJ,M,XP,P,PP) puts $P_n^m(\cos\theta)$ in $P(L2+m\cdot NJ-(m-1)\cdot m/2+n-m+1)$ and $\frac{dP_n^m(\cos\theta)}{d\theta}$ in $PP(L4+m\cdot NJ-(m-1)\cdot m/2+n-m+1)$ where

$$L2 = (L-1) \times L5$$

$$L4 = (LD-1) \times L5$$

$$L5 = M*NJ-M*(M-1)/2$$

$$0 \le m \le M-1$$

$$m \le n \le NJ-1$$

In the main program, the nested Do loops 232 and 233 multiply $P_n^m(\cos \theta)$ and $\frac{d}{d\theta} P_n^m(\cos \theta)$ by the factor $(2n+1) \frac{(n-m)!}{(n+m)!}$ appearing in (33).

The logic between statements 234 and 210 calculates spherical Bessel functions $j_n(kr')$ and $y_n(kr')$ and the associated Legendre polynomials $P_n^m(\cos \theta')$ if necessary. The spherical Bessel functions $j_n(kr')$ and $y_n(kr')$ have been previously calculated for $n=0,1,2...N3-1$ and the associated Legendre functions $P_n^m(\cos \theta')$ for $m=0,1,2...M3-1$ and $n=m,m+1,...N3-1$.

The integrations (30), (31) and (32) are done by sampling at KG=NP-1 points of which the Jth is located midway between the Jth and $(J+1)^{th}$ data point on the generating curve. This J is the index of Do loop 212. In Do loop 213,

$$U1(I) = \begin{cases} h_n^{(2)}(kr')j_n(k\rho) & r' > \rho \\ \\ h_n^{(2)}(k\rho)j_n(kr') & r' < \rho \end{cases}$$

$$U2(I) = \begin{cases} h_n^{(2)}(kr') \dfrac{d \, j_n(k\rho)}{d\rho} & r' > \rho \\ \\ \dfrac{d}{d\rho} h_n^{(2)}(k\rho)j_n(kr') & r' < \rho \end{cases}$$

where $n = I-1$. In Do loop 212,

$$G1 = G_{m-1} \qquad\qquad G4 = \frac{\partial}{\partial \theta} G_m$$

$$G2 = \frac{\partial}{\partial \rho} G_{m-1} \qquad\qquad G5 = G_{m+1}$$

$$G3 = G_m \qquad\qquad G6 = \frac{\partial}{\partial \rho} G_{m+1}$$

where G_m is defined by (33). In Do loop 226,

31

$$V1(J) = \frac{4}{\eta} V^t_{mJ}$$

$$V1(J2) = \frac{4}{\eta} V^\phi_{mJ}$$

where V^t_{mJ} and V^ϕ_{mJ} are given by (30) with $I\ell_x = 1$. Similarly, V2 and V3 are given by (31) with $I\ell_y = 1$ and by (32) with $I\ell_z = 1$.

If

$$KV > 90$$
$$NP > 41$$
$$M1 > 4$$
$$N1 > 14$$

some variables may require more space. These variables are listed along with their minimum dimensions. In the subroutine LEG,

DIMENSION PC(M1+4),PS(N1+1)

In the main program,

COMPLEX   G1(KG),G2(KG),G3(KG),G4(KG),G5(KG),G6(KG),U1(N1+1),
                  U2(N1+1),V(NM2),V1(NM2),V2(NM2),V3(NM2)

DIMENSION   RH(NP),ZH(NP),DH(KG),R(KG),ZS(KG),SV(KG),CV(KG)
                  T(4×NM),TP(4×NM),TR(4×NM),M1(KV),N1(KV),XR(KV),XP(KV),
                  XZ(KV),UR(KV),UP(KV),UZ(KV),BJ1(L1),BJ2(L1),
                  BJ3(L1),BY1(L1),BY2(L1),BY3(L1),P1(L2),P3(L1*KG),
                  PS(N1+M1+2),P2(L2)

where

$$KG = NP-1$$
$$NM2 = NP-3$$
$$L1 = KG×(N1+1)$$
$$L2 = (M1+2)*(N1+1)-(M1+2)*(M1+1)/2$$

If N1+M1>20, statement 245 must changed so that J1 is at least as large as the maximum value of N1+M1+1.

The subroutine BES(L,LD,ID,NJ,XJ,BJ,BJP,BY,BYP) puts j_n(XJ) in BJ(L1+1) through BJ(L1+NJ) where n = 0,1,2,...NJ-1 and L1=(L-1)×NJ. If XJ $\leq$ .001, j_n(XJ) is approximated by

$$j_n(XJ) = \begin{cases} 1 & n=0 \\ 0 & n=1,2,3,...NJ-1 \end{cases}$$

before returning to the main program. If XJ > .001, y_n(XJ) is put in BY(L1+1) through BY(L1+NJ). If both XJ > .001 and ID $\neq$ 2, j_n'(XJ) and y_n'(XJ) are put in BJP(L3+1) through BJP(L3+NJ) and BYP(L3+1) through BYP(L3+NJ) respectively where n=0,1,2...NJ-1 and L3=(LD-1)*NJ.

If XJ $\geq$ 15, j_n(XJ) is computed from

$$j_0(z) = \frac{\sin z}{z}$$

$$j_1(z) = \frac{\sin z}{z^2} - \frac{\cos z}{z}$$

$$j_{n+1}(z) = \frac{(2n+1)}{z} j_n(z) - j_{n-1}(z), \quad n=1,2,...NJ-2$$

where z = XJ. If XJ < 15, statement 11 sets NBJ=XJ+22 and j_n(XJ) is computed from

$$j_N(z) = 0$$

$$j_{N-1}(z) = 1$$

$$j_{n-1}(z) = \frac{2n+1}{z} j_n(z) - j_{n+1}(z), \quad n=N-1,N-2,...1$$

and normalized according to either $j_0(z) = \frac{\sin z}{z}$ or $j_1(z) = \frac{\sin z}{z^2} - \frac{\cos z}{z}$, whichever is largest in magnitude. Here, N=NBJ-1. When statement 15 is reached, the spherical Bessel function of the second kind y_n(z) is computed from

$$y_0(z) = - \frac{\cos z}{z}$$

$$y_1(z) = - \frac{\cos z}{z^2} - \frac{\sin z}{z}$$

$$y_{n+1}(z) = \frac{2n+1}{z} y_n(z) - y_{n-1}(z), \quad n=1,2,3,\ldots NJ-2$$

If $ID \neq 2$, $j_n'(z)$ and $y_n'(z)$ are computed from

$$j_0'(z) = - j_1(z)$$

$$j_n'(z) = \frac{nj_{n-1}(z) - (n+1) j_{n+1}(z)}{2n+1}, \quad n=1,2,\ldots NJ-1$$

which is also valid for $y_n'(z)$.

The subroutine LEG(L,LD,ID,NJ,M,XP,P,PP) calculates associated Legendre polynomials

$$P_n^m(XP) \quad , \quad \begin{cases} m = 0,1,2,\ldots M-1 \\ n = m, m+1, \ldots NJ-1 \end{cases}$$

By definition,

$$P_n^m(u) = \frac{(1-u^2)^{\frac{m}{2}}}{2^n n!} \frac{d^{m+n}}{du^{m+n}} (u^2 - 1)^n$$

so that

$$P_m^m(u) = [1.3.5 \ldots (2m-1)] (1-u^2)^{\frac{m}{2}}$$

$$P_{m+1}^m(u) = [1.3.5 \ldots (2m+1)] u(1-u^2)^{\frac{m}{2}} .$$

Do loop 7 puts $[1.3.5 \ldots (2n-1)]$ in PC(n+1). By definition PC(1) = 1. Do loop 3 calculates $P_n^m(u)$ for m=J-1. $P_n^m(u)$ occupies first the dimensioned variable PS but is later transferred to P(J2) where

$$J2 = (L-1)*(M*NJ - M*(M-1)/2) + m*NJ - \frac{m(m-1)}{2} + n-m+1 .$$

34

When $n \geq m+2$, P_n^m is calculated from

$$P_n^m(u) = 2u\, P_{n-1}^m - P_{n-2}^m + \frac{(2m-1)}{n-m}\,(u\, P_{n-1}^m - P_{n-2}^m)$$

If ID $\neq$ 2, Do loop 5 calculates the derivative of the associated Legendre polynomials

$$\frac{d}{d\theta}\, P_n^m(\cos\theta), \qquad \begin{array}{l} m = 0,1,2,\ldots\ M-1 \\[4pt] n=m,\ m+1,\ \ldots\ NJ-1 \end{array}$$

When $n \geq m+1$,

$$\frac{d}{d\theta}\, P_n^m\,(\cos\theta) = - P_n^{m+1} \qquad\qquad\qquad m=0$$

$$\frac{d}{d\theta}\, P_n^m\,(\cos\theta) = \tfrac{1}{2}[(n+m)(n-m+1)P_n^{m-1} - P_n^{m+1}] \qquad m=1,2,\ldots$$

and when $n = m$,

$$\frac{d}{d\theta}\, P_m^m\,(\cos\theta) = 0 \qquad\qquad m=0$$

$$\frac{d}{d\theta}\, P_m^m\,(\cos\theta) = mP_m^{m-1} \qquad\qquad m=1,2,\ldots$$

The quantity $\dfrac{dP_n^m}{d\theta}\,(\cos\theta)$ for $\cos\theta$ = XP is stored in PP(J2) where

$$J2 = (LD-1)*(M*NJ - M*(M-1)/2) + M*NJ - \frac{M(M-1)}{2} + n-M+1 \ .$$

The second program uses the generalized admittance matrices $[Y_m]$ and voltage matrices $[V_m]^t$ to compute the induced current $\underset{\sim}{J}$ and gain pattern for a dipole $I\underset{\sim}{\ell}$ radiating near a body of revolution. The program which calculates $[Y_m]$ is listed in Appendix A of a previous report [4].

Punched card data is read early in the main program according to

```
88   READ(1,51,END=52)KV,NP,NMAX,NT,BK

51   FORMAT(4I3,E14.7)
     READ(1,53)(RH(I),I=1,NP)
     READ(1,53)(ZH(I),I=1,NP)
```

The variables KV,NP,BK,RH, and ZH have the same meaning as in the first program. NMAX is one more than the maximum value of M encountered in equation (34). The gain is computed at $\theta = (L-1) \dfrac{\pi}{NT-1}$, $L = 1,2,\ldots NT$ in radians in both the $\phi = 0$ and $\phi = \pi$ planes. The admittance matrices are read from direct access data set 6 according to

```
     REWIND 6
     DO 61 J=1, NMAX
     J2 = (J-1)*NZ+1
     J3 = J2 + NZ-1
     READ(6)(Y(I),I=J2,J3)
61   CONTINUE
```

where $NZ = (NP-3) \times (NP-3)$.

More punched card data is read according to

```
     DO 62 K=1,KV
     READ(1,63)NX,(KK1(I),I=1,NX)
63   FORMAT (10I3)
     READ(1,64)XR,XZ,UR,UP,UZ
64   FORMAT(5F9.4)
62   CONTINUE
```

For the Kth dipole, the Ith term to be treated in (34) is for m = (KK1(I). The −m terms of (34) are combined with the +m terms so that KK1(I) ≥ 0. If the m=0 term is considered, it must be treated first so that KK1(1) is the only KK1 that can ever be zero. The variables XR,XZ,UR,UP, and UZ correspond to the dimensioned variables of the same name in the first program. The variable XP is missing because only dipoles in the $\phi = 0$ plane are considered. The data UR, UP, and UZ is restricted such that either UP = 0 or UR = UZ = 0. The sample data for the second program is for the same dipole outside the same cone-sphere as in the first program.

For UP = 0, equation (15) becomes

$$\underset{\sim}{J} = \underset{\sim}{u}_t \sum_{m=0}^{M} \sum_{i=1}^{N} \varepsilon_m I_{mi}^t f_i(t) \cos m\phi + \underset{\sim}{u}_\phi \sum_{m=1}^{M} \sum_{i=1}^{N} 2j I_{mi}^\phi f_i(t) \sin m\phi$$

For UR = UZ = 0, equation (15) becomes

$$\underset{\sim}{J} = \underset{\sim}{u}_t \sum_{m=1}^{M} \sum_{i=1}^{N} 2j I_{mi}^t f_i(t) \sin m\phi + \underset{\sim}{u}_\phi \sum_{m=0}^{M} \sum_{i=1}^{N} \varepsilon_m I_{mi}^\phi f_i(t) \cos m\phi$$

For UP = 0, the current printed immediately after statement 256 is the matrix

$$[\varepsilon_m I_{mi}^t] \quad [2j I_{mi}^\phi]$$

For UR = UZ = 0, the current printed is the matrix

$$[2j I_{mi}^t] \quad [\varepsilon_m I_{mi}^\phi]$$

The mutual impedance printed is Z_{mut} appearing in (47). The scattered far electric field printed is either $\underset{\sim}{E}^S \cdot \underset{\sim}{u}_\theta$ normalized to $\dfrac{-j\omega\mu e^{-jkr}}{4\pi r}$ in the plane $\phi = 0, \pi$ when UP = 0 or $\underset{\sim}{E}^S \cdot \underset{\sim}{u}_\phi$ in the plane $\phi = 0, \pi$ normalized to $\dfrac{-j\omega\mu e^{-jkr}}{4\pi r}$ when UR = UP = 0. The write statements following statement 258 are for $\underset{\sim}{E}^S \cdot \underset{\sim}{u}$ when $\phi = 0$, $\underset{\sim}{E}^S \cdot \underset{\sim}{u}$ when $\phi = \pi$, $|\underset{\sim}{E}^S \cdot \underset{\sim}{u}|$ when $\phi = 0$ and $|\underset{\sim}{E}^S \cdot \underset{\sim}{u}|$ when $\phi = \pi$. In all four write statements, L indicates $\theta = \dfrac{(L-1)*\pi}{NT-1}$. The write statements following statement 259 are for the gain when $\phi = 0$, π. The gain, defined by (43), is also plotted at the end of the main program.

The variables DH, R, ZS, SV, CV, T and TR appearing early in the main program are the same as those in the first program. Statement 263 inside Do loop 61 puts $[R_m]^\theta$ of equation (42) in VR(J1) through VR(J1 + NM2-1) and $[R_m]^\phi$ in VR(J1+NM2) through VR(J1+NM4-1) where

$$m = J-1$$
$$J1 = 1 + NM4 \times NT*(J-1)$$
$$NM2 = NP-3$$
$$NM4 = NM2*2$$

The subroutine PLANE (VVR, THR, NT) is described in Section V of a previous report [4].

The index K of Do loop 62 indicates the Kth dipole. In Do loop 68, the index J obtains m = KK1(J) in equation (15). Do loop 70 puts the I matrix on the left hand side of (17) in TI(1) through TI(NM2). In Do loop 84, E(L) is proportional to $\underset{\sim}{E}^s \cdot \underset{\sim}{u}$ for ϕ = 0 and E(L2) is proportional to $\underset{\sim}{E}^s \cdot \underset{\sim}{u}$ for $\phi = \pi$ where L2 = L + NT and $\underset{\sim}{u} = \underset{\sim}{u}_\theta$ or $\underset{\sim}{u}_\phi$ depending on whether UP = 0 or UR = UZ = 0. The index L indicates $\theta = \dfrac{(L-1)*\pi}{NT-1}$. Do loop 243 facilitates calculation of U2 which is the negative of the right hand side of (34) with $I\ell_r$ replaced by $I\underset{\sim}{\ell}$. In statement 264

$$P2 = k \sqrt{\frac{\eta}{4\pi P}}$$

where P is the total power radiated. P2 is required to normalize the gain.

The logic between statements 92 and 94 computes the dipole far electric field normalized to $\dfrac{-j\omega\mu e^{-jkr}}{4\pi r}$. $\underset{\sim}{E}^d \cdot \underset{\sim}{u}$ of (45) for ϕ = 0 resides in E1(J) and $\underset{\sim}{E}^d \cdot \underset{\sim}{u}$ for $\phi = \pi$ resides in E1(J+NT). Here, $\underset{\sim}{u} = \underset{\sim}{u}_\theta$ or $\underset{\sim}{u}_\phi$ depending on whether UP = 0 or UR = UZ = 0. Upon exit from Do loop 96, the gain for ϕ = 0 and $\theta = \dfrac{(J-1)*\pi}{NT-1}$ is stored in E3(J). The gain for $\phi = \pi$ and $\theta = \dfrac{(J-1)\times\pi}{NT-1}$ is stored in E3(J+NT). The gain is plotted after it is printed. In Do loop 244, E3(J) and E4(J) are respectively the abscissa x and ordinate y of the gain pattern for ϕ = 0. E3(J+NT) and E4(J+NT) are for $\phi = \pi$. Statements 265 and 266 plot the gain for ϕ = 0 and $\phi = \pi$ respectively. Statements 267 and 268 draw the x and y axes. Do loop 245 puts tick marks on the x axis and Do loop 246 puts tick marks on the y axis. Do loop 253 labels the x axis from 1 to 5.

If the data NP, NMAX, or NT is changed, some dimensioned variables may require more space. These variables are listed along with their minimum dimensions.

```
COMPLEX     VR(NT×NMAX*NM4),Y(NZ),E(NT2),E1(NT2),V(NM2),
            TI(NM2)
DIMENSION   RH(NP),ZH(NP),DH(NP-1),TH(NT),KK1(NMAX),
            S6(NT),S7(NT),E3(NT2),E4(NT2)
COMMON      R(NP-1),ZS(NP-1),SV(NP-1),CV(NP-1),T(NM4),
            TR(NM4)
where       NM2 = NP-3
            NM4 = 2×(NP-3)
            NZ  = (NP-3)*(NP-3)
            NT2 = NT×2
```

The common statement in the subroutine PLANE must remain exactly the same as in the main program.

VII. COMPUTER PROGRAMS AND SAMPLE OUTPUT

A. Program for Voltage Excitation

```
//                 (0034,EE,4,2,44),'MAUTZ,JOE',MSGLEVEL=1
// EXEC FORTGCLG,PARM.FORT='MAP'
//FORT.SYSIN DD *
      SUBROUTINE BES(L,LD,ID,NJ,XJ,BJ,BJP,BY,BYP)
      DIMENSION BJ(1),BJP(1),BY(1),BYP(1),BS(40)
      L1=(L-1)*NJ
      L3=(LD-1)*NJ
    6 IF(XJ-1.E-3) 3,3,4
    3 J1=L1+1
      J2=L1+NJ
      DO 5 J=J1,J2
      BJ(J)=0.
    5 CONTINUE
      BJ(1)=1.
      RETURN
    4 SN=SIN(XJ)
      CS=COS(XJ)
      IF(XJ-15.) 11,12,12
   12 BJ(L1+1)=SN/XJ
      BJ(L1+2)=(BJ(L1+1)-CS)/XJ
      DO 14 I=3,NJ
      I3=L1+I
      I2=I3-1
      I1=I3-2
      BJ(I3)=FLOAT(2*I-3)/XJ*BJ(I2)-BJ(I1)
   14 CONTINUE
      B3=FLOAT(2*NJ-1)/XJ*BJ(I3)-BJ(I2)
      GO TO 15
   11 NBJ=XJ+22.
      BS(NBJ)=0.
      BS(NBJ-1)=1.
      NBJ2=NBJ-2
      DO 193 I=1,NBJ2
      I2=NBJ-I
      I3=I2+1
      I1=I2-1
      FI=FLOAT(2*I1+1)/XJ
      BS(I1)=BS(I2)*FI-BS(I3)
  193 CONTINUE
      B1=SN/XJ
      B2=B1/XJ-CS/XJ
      IF(ABS(B1)-ABS(B2))1,2,2
    2 BB=B1/BS(1)
      GO TO 9
    1 BB=B2/BS(2)
    9 DO 194 I=1,NJ
      I1=L1+I
      BJ(I1)=BS(I)*BB
  194 CONTINUE
      B3=BS(NJ+1)*BB
   15 BY(L1+1)=-CS/XJ
      BY(L1+2)=(BY(L1+1)-SN)/XJ
      DO 64 I=3,NJ
      I3=L1+I
      I2=I3-1
      I1=I3-2
      BY(I3)=FLOAT(2*I-3)/XJ*BY(I2)-BY(I1)
   64 CONTINUE
      B4=FLOAT(2*NJ-1)/XJ*BY(I3)-BY(I2)
      IF(ID.EQ.2) RETURN
```

40

```
      NJ1=NJ-1
      J1=L3+1
      J2=L1+2
      BJP(J1)=-BJ(J2)
      BYP(J1)=-BY(J2)
      DO 65 J=2,NJ1
      J2=L3+J
      J1=L1+J-1
      J3=J1+2
      FJ=2*(2*J-1)
      BJP(J2)=.5*(BJ(J1)-BJ(J3))-(BJ(J1)+BJ(J3))/FJ
      BYP(J2)=.5*(BY(J1)-BY(J3))-(BY(J1)+BY(J3))/FJ
   65 CONTINUE
      FJ=FJ+4.
      J2=J2+1
      J1=J1+1
      BJP(J2)=.5*(BJ(J1)-B3)-(BJ(J1)+B3)/FJ
      BYP(J2)=.5*(BY(J1)-B4)-(BY(J1)+B4)/FJ
      RETURN
      END
      SUBROUTINE LEG(L,LD,ID,NJ,M,XP,P,PP)
      DIMENSION PC(8),P(1),PP(1),PS(20)
      PC(1)=1.
      M1=M+1
      DO 7 J=1,M1
      PC(J+1)=PC(J)*FLOAT(2*J-1)
    7 CONTINUE
      L5=M*NJ-M*(M-1)/2
      L2=(L-1)*L5
      L4=(LD-1)*L5
      X2=ABS(1.-XP*XP)
      X1=SQRT(X2)
      DO 3 J=1,M1
      M2=L2+(J-1)*NJ-(J-2)*(J-1)/2
      X3=1.
      IF(J.NE.1) X3=X1**(J-1)
      PS(1)=PC(J)*X3
      PS(2)=PC(J+1)*XP*X3
      IF(J.EQ.M1) GO TO 14
      P(M2+1)=PS(1)
      P(M2+2)=PS(2)
   14 NJ1=NJ-J+1
      DO 4 I=3,NJ1
      I1=I-2
      I2=I-1
      PS(I)=2.*XP*PS(I2)-PS(I1)+FLOAT(2*J-3)/FLOAT(I2)*(XP*PS(I2)-PS(I1)
     1)
      IF(J.EQ.M1) GO TO 4
      J2=M2+I
      P(J2)=PS(I)
    4 CONTINUE
    3 CONTINUE
      IF(ID.EQ.2) RETURN
      DO 5 J=1,M
      M2=L4+(J-1)*NJ-(J-2)*(J-1)/2
      M3=M2+L2-L4
      NJ1=NJ-J+1
      DO 6 I=2,NJ1
      J2=M2+I
      J1=M3+I-NJ+J-1
```

```
      J3=M3+I+NJ-J
      IF(J.NE.1.AND.J.NE.M) GO TO 8
      IF(J.NE.1) GO TO 12
      PP(J2)=-P(J3)
      GO TO 6
12    PP(J2)=.5*(FLOAT(I*(2*J+I-3))*P(J1)-PS(I-1))
      GO TO 6
8     PP(J2)=.5*(FLOAT(I*(2*J+I-3))*P(J1)-P(J3))
6     CONTINUE
      J2=M2+1
      J1=M3-NJ+J
      IF(J.NE.1) GO TO 13
      PP(J2)=0.
      GO TO 5
13    PP(J2)=.5*FLOAT(2*J-2)*P(J1)
5     CONTINUE
      RETURN
      END
      COMPLEX U,G1(40),G2(40),G3(40),G4(40),G5(40),G6(40),U1(17),U2(17)
      COMPLEX U3,C1,C2,C3,U4,U5,U6,U7,U8,U9,V(38),V1(38),V2(38),V3(38)
      DIMENSION RH(41),ZH(41),DH(40),R(40),ZS(40),SV(40),CV(40),T(76)
      DIMENSION TP(76),TR(76),M1(90),N1(90),XR(90),XP(90),XZ(90),UR(90)
      DIMENSION UP(90),UZ(90),BJ1(600),BJ2(600),BJ3(600),BY1(600)
      DIMENSION BY2(600),BY3(600),P1(87),P2(87),P3(3000),PS(22)
      ETA=376.730
      PI=3.141593
      U=(0.,1.)
      PR=PI/180.
50    READ(1,51,END=52) KV,NP,BK
51    FORMAT(2I3,E14.7)
      READ(1,53)(RH(I),I=1,NP)
      READ(1,53)(ZH(I),I=1,NP)
53    FORMAT(10F8.4)
76    WRITE(3,54) KV,NP,BK
54    FORMAT(1X//' KV=',I3,' NP=',I3,' BK=',E14.7)
      WRITE(3,55)
55    FORMAT(1X/' RH')
      WRITE(3,46)(RH(I),I=1,NP)
46    FORMAT(1X,10F8.4)
      WRITE(3,56)
56    FORMAT(1X/' ZH')
      WRITE(3,46)(ZH(I),I=1,NP)
      KL=1
126   IF((RH(1)-RH(NP)).NE.0..OR.(ZH(1)-ZH(NP)).NE.0.) GO TO 58
      KL=0
      RH(NP+1)=RH(2)
      ZH(NP+1)=ZH(2)
      RH(NP+2)=RH(3)
      ZH(NP+2)=ZH(3)
      NP=NP+2
58    DO 57 I=2,NP
      I2=I-1
      RR1=RH(I)-RH(I2)
      RR2=ZH(I)-ZH(I2)
      DH(I2)=SQRT(RR1*RR1+RR2*RR2)
      R(I2)=.5*(RH(I)+RH(I2))
      ZS(I2)=.5*(ZH(I)+ZH(I2))
      SV(I2)=RR1/DH(I2)
      CV(I2)=RR2/DH(I2)
57    CONTINUE
```

```
      NM=(NP-3)/2
      NM2=NM*2
      NM4=NM*4
      KG=NP-1
      BK2=BK*BK
      DO 74 J=1,NM
      J2=2*(J-1)+1
      J3=J2+1
      J4=J3+1
      J5=J4+1
      J6=4*(J-1)+1
      J7=J6+1
      J8=J7+1
      J9=J8+1
      DEL1=DH(J2)+DH(J3)
      DEL2=DH(J4)+DH(J5)
      T(J6)=DH(J2)*DH(J2)/2./DEL1
      T(J7)=DH(J3)*(DH(J2)+DH(J3)/2.)/DEL1
      T(J8)=DH(J4)*(DH(J5)+DH(J4)/2.)/DEL2
      T(J9)=DH(J5)*DH(J5)/2./DEL2
      TP(J6)=DH(J2)/DEL1
      TP(J7)=DH(J3)/DEL1
      TP(J8)=-DH(J4)/DEL2
      TP(J9)=-DH(J5)/DEL2
   74 CONTINUE
      DO 75 J=1,NM4
      TR(J)=T(J)
   75 CONTINUE
  115 IF(KL.EQ.0) GO TO 78
      IF(RH(1)) 77,23,77
   77 DEL1=DH(1)+DH(2)
      TR(1)=DH(1)*(1.+(DH(2)+DH(1)/2.)/DEL1)
      TR(2)=DH(2)*(1.+DH(2)/2./DEL1)
   23 IF(RH(NP)) 79,78,79
   79 J1=(NM-1)*4+3
      J2=J1+1
      DEL2=DH(NP-2)+DH(NP-1)
      TR(J1)=DH(NP-2)*(1.+DH(NP-2)/2./DEL2)
      TR(J2)=DH(NP-1)*(1.+(DH(NP-2)+DH(NP-1)/2.)/DEL2)
   78 M2=-1
      N2=-1
      M3=-1
      N3=-1
      M1(1)=-1
      N1(1)=-1
      XR(1)=1.E+10
      X7(1)=XR(1)
  245 J1=21
      PS(1)=1.
      DO 231 J=1,J1
      J2=J+1
      PS(J2)=PS(J)*J
  231 CONTINUE
      DO 200 K=1,KV
      K1=K+1
      READ(1,201)M1(K1),N1(K1),XR(K1),XP(K1),X7(K1),UR(K1),UP(K1),U7(K1)
  201 FORMAT(2I3,6F9.4)
      WRITE(3,203)
  203 FORMAT('0 M1 N1',4X,'XR',7X,'XP',7X,'X7',7X,'UR',7X,'UP',7X,'U7')
      WRITE(3,202) M1(K1),N1(K1),XR(K1),XP(K1),X7(K1),UR(K1),UP(K1),U7(K
```

```
      11)
  202 FORMAT(1X,2I3,6F9.4)
      X4=M1(K1)*XP(K1)*PR
  246 U4=ETA/4.*(COS(X4)-U*SIN(X4))
      C1=UR(K1)*U4
      C2=UP(K1)*U4
      C3=UZ(K1)*U4
      X5=ABS(XR(K1)-XR(K))+ABS(XZ(K1)-XZ(K))
      IF(IABS(M1(K1)-M1(K))+IABS(N1(K1)-N1(K))+X5) 235,235,236
  236 N4=N1(K1)+1
      M4=M1(K1)
      M5=M4+1
      M6=M5+1
      IF((N1(K1)+1-N2).LE.0) GO TO 204
      N2=N1(K1)+1
      DO 208 J=1,KG
      XJ=BK*R(J)
      CALL BES(J,J,1,N2,XJ,BJ1,BJ2,BY1,BY2)
  208 CONTINUE
      GO TO 238
  204 IF((M1(K1)+2-M2).LE.0) GO TO 234
  238 M2=M1(K1)+2
  244 CALL LEG(1,1,1,N2,M2,0.,P1,P2)
      DO 232 J=1,M2
      J2=(J-1)*N2-J*(J-1)/2
      DO 233 I=J,N2
      J1=J2+I
      X6=(2*I-1)*PS(I-J+1)/PS(I+J-1)
      P1(J1)=P1(J1)*X6
      P2(J1)=P2(J1)*X6
  233 CONTINUE
  232 CONTINUE
  234 IF(X5) 206,206,240
  240 M3=-1
      N3=-1
  206 IF((N1(K1)+1-N3).LE.0) GO TO 207
      N3=N1(K1)+1
      M3=M1(K1)+2
      DO 229 J=1,KG
      Z1=XZ(K1)-ZS(J)
      XJ=SQRT(Z1*Z1+XR(K1)*XR(K1))
      XJ1=BK*XJ
      CALL BES(J,J,2,N3,XJ1,BJ3,BJ2,BY3,BY2)
      XJ1=Z1/XJ
      CALL LEG(J,J,2,N3,M3,XJ1,P3,P2)
  229 CONTINUE
      GO TO 210
  207 IF((M1(K1)+2-M3).LE.0) GO TO 210
      M3=M1(K1)+2
      DO 211 J=1,KG
      Z1=XZ(K1)-ZS(J)
      XJ=Z1/SQRT(Z1*Z1+XR(K1)*XR(K1))
      CALL LEG(J,J,2,N3,M3,XJ,P3,P2)
  211 CONTINUE
  210 J5=-M5*(M5-1)/2
      DO 212 J=1,KG
      J3=(M3*N3-M3*(M3-1)/2)*(J-1)
      G1(J)=0.
      G2(J)=0.
      G3(J)=0.
```

```
      G4(J)=0.
      G5(J)=0.
      G6(J)=0.
      Z1=XZ(K1)-ZS(J)
      X2=SQRT(Z1*Z1+XR(K1)*XR(K1))
      DO 213 I=1,N4
      J1=I+(J-1)*N2
      J2=I+(J-1)*N3
      IF(R(J)-X2) 215,214,214
  214 X3=BJ1(J1)
      X4=BJ2(J1)
      IF(ABS(X3)+ABS(X4)-1.E-15) 216,217,217
  216 X3=0.
      X4=0.
  217 U1(I)=BJ3(J2)*(X3-U*BY1(J1))
      U2(I)=BJ3(J2)*BK*(X4-U*BY2(J1))
      GO TO 213
  215 X3=BJ3(J2)
      IF(ABS(X3)-1.E-15) 218,219,219
  218 X3=0.
  219 U3=X3-U*BY3(J2)
      U1(I)=BJ1(J1)*U3
      U2(I)=BJ2(J1)*BK*U3
  213 CONTINUE
      J4=(M5-1)*N2+J5
      J6=J3+(M5-1)*N3+J5
      DO 220 I=M5,N4
      J1=J4+I
      J2=J6+I
      G3(J)=P1(J1)*P3(J2)*U1(I)+G3(J)
      G4(J)=P2(J1)*P3(J2)*U1(I)+G4(J)
  220 CONTINUE
      J4=J4+N2-M5
      J6=J6+N3-M5
      DO 221 I=M6,N4
      J1=J4+I
      J2=J6+I
      G5(J)=P1(J1)*P3(J2)*U1(I)+G5(J)
      G6(J)=P1(J1)*P3(J2)*U2(I)+G6(J)
  221 CONTINUE
      IF(M4) 222,223,222
  223 G1(J)=G5(J)
      G2(J)=G6(J)
      GO TO 212
  222 J4=J4-2*(N2-M5)-1
      J6=J6-2*(N3-M5)-1
      DO 225 I=M4,N4
      J1=J4+I
      J2=J6+I
      G1(J)=P1(J1)*P3(J2)*U1(I)+G1(J)
      G2(J)=P1(J1)*P3(J2)*U2(I)+G2(J)
  225 CONTINUE
  212 CONTINUE
      DO 226 J=1,NM
      J2=J+NM
      V1(J)=0.
      V2(J)=0.
      V3(J)=0.
      V1(J2)=0.
      V2(J2)=0.
```

```
      V3(J2)=0.
      DO 227 I=1,4
      J5=(J-1)*4+I
      J4=(J-1)*2+I
      X4=(M4-1)/R(J4)
      X5=M4/R(J4)
      X6=M5/R(J4)
      U4=BK2*(G5(J4)-G1(J4))
      U5=BK2*(G5(J4)+G1(J4))
      U6=G6(J4)-G2(J4)
      U7=G6(J4)+G2(J4)
      U8=X6*G5(J4)-X4*G1(J4)
      U9=X6*G5(J4)+X4*G1(J4)
      V1(J)=-T(J5)*SV(J4)*U5+TP(J5)*(U7+U8)+V1(J)
      V2(J)=(-T(J5)*SV(J4)*U4+TP(J5)*(U6+U9))*U+V2(J)
      V3(J)=-BK2*T(J5)*CV(J4)*G3(J4)-TP(J5)/R(J4)*G4(J4)+V3(J)
      V1(J2)=(U4-X5*(U7+U8))*U*TR(J5)+V1(J2)
      V2(J2)=(-U5+X5*(U6+U9))*TR(J5)+V2(J2)
      V3(J2)=X5/R(J4)*TR(J5)*G4(J4)*U+V3(J2)
  227 CONTINUE
      V3(J)=2.*V3(J)
      V3(J2)=2.*V3(J2)
  226 CONTINUE
  235 DO 237 J=1,NM2
      V(J)=C1*V1(J)+C2*V2(J)+C3*V3(J)
  237 CONTINUE
      WRITE(3,243)
  243 FORMAT('0VOLTAGE MATRIX')
      WRITE(3,228)(V(J),J=1,NM2)
  228 FORMAT(1X,10G11.4)
      WRITE(2,241)(V(J),J=1,NM2)
  241 FORMAT(7E11.4)
  200 CONTINUE
      GO TO 50
   52 STOP
      END
/*
//GO.SYSIN DD *
004041 0.4659995E+00
  0.0      0.0868  0.1736  0.2605  0.3473  0.4341  0.5209  0.6078  0.6946  0.7814
  0.8682  0.9551  1.0419  1.1287  1.2155  1.3024  1.3892  1.4760  1.5628  1.6497
  1.7365  1.8233  1.9101  1.9970  2.0838  2.1706  2.2574  2.3442  2.4311  2.5179
  2.6047  2.6837  2.6863  2.5969  2.4184  2.1570  1.8216  1.4238  0.9772  0.4971
 -0.0000
  0.0      0.4924  0.9848  1.4772  1.9696  2.4620  2.9544  3.4468  3.9392  4.4316
  4.9240  5.4164  5.9088  6.4013  6.8937  7.3861  7.8785  8.3709  8.8633  9.3557
  9.8481 10.3405 10.8329 11.3253 11.8177 12.3101 12.8025 13.2949 13.7873 14.2797
 14.7721 15.2657 15.7650 16.2562 16.7225 17.1478 17.5177 17.8195 18.0427 18.1798
 18.2260
003014    4.3615    0.0000    5.3235    1.0000    0.0000    0.0000
000014    4.3615    0.0000    5.3235    1.0000    0.0000    0.0000
001014    4.3615    0.0000    5.3235    1.0000    0.0000    0.0000
002014    4.3615    0.0000    5.3235    1.0000    0.0000    0.0000
/*
```

B. Sample Output

KV= 4 NP= 41 BK= 0.4659995E 00

RH
```
0.0      0.0868   0.1736   0.2605   0.3473   0.4341   0.5209   0.6078   0.6946   0.7814
0.8682   0.9551   1.0419   1.1287   1.2155   1.3024   1.3892   1.4760   1.5628   1.6497
1.7365   1.8233   1.9101   1.9970   2.0838   2.1706   2.2574   2.3442   2.4311   2.5179
2.6047   2.6837   2.6863   2.5969   2.4184   2.1570   1.8216   1.4238   0.9772   0.4971
0.0
```

ZH
```
0.0      0.4924   0.9848   1.4772   1.9696   2.4620   2.9544   3.4468   3.9392   4.4316
4.9240   5.4164   5.9088   6.4013   6.8937   7.3861   7.8785   8.3709   8.8633   9.3557
9.8481   10.3405  10.8329  11.3253  11.8177  12.3101  12.8025  13.2949  13.7873  14.2797
14.7721  15.2657  15.7650  16.2562  16.7225  17.1478  17.5177  17.8195  18.0427  18.1798
18.2260
```

```
M1 N1    XR       XP       XZ       UR       UP       UZ
3 14     4.3615   0.0      5.3235   1.0000   0.0      0.0
```

VOLTAGE MATRIX
```
-0.3105E-03-0.7578E-03-0.1201E-02-0.7585E-02-0.2892E-02-0.4317E-01-0.5469E-02-0.1431    -0.8912E-02-0.2367
-0.1305E-01-0.1274    -0.1762E-01 0.6862E-01-0.2223E-01 0.1018    -0.2645E-01 0.3994E-01-0.2983E-01-0.6448E-02
-0.3199E-01-0.2235E-01-0.3263E-01-0.2171E-01-0.3162E-01-0.1489E-01-0.2901E-01-0.6747E-02-0.2488E-01-0.1663E-02
-0.2102E-01-0.1251E-01-0.1997E-01-0.2046E-01-0.1507E-01-0.1421E-01-0.5823E-02-0.4817E-02 0.3772E-02-0.1788E-02
 0.3112E-01-0.7132E-02 0.1535    -0.1723E-01 0.5114    -0.3226E-01 1.108    -0.5146E-01 1.481    -0.7307E-01
 1.241    -0.9452E-01 0.7248    -0.1128     0.3403    -0.1251     0.1362    -0.1289     0.3254E-01-0.1228
-0.2587E-01-0.1068    -0.6156E-01-0.8211E-01-0.8178E-01-0.5145E-01-0.8812E-01-0.1837E-01-0.7648E-01 0.1055E-01
-0.4842E-01 0.2320E-01-0.2127E-01 0.1775E-01-0.5497E-02 0.6368E-02
```

```
M1 N1    XR       XP       XZ       UR       UP       UZ
0 14     4.3615   0.0      5.3235   1.0000   0.0      0.0
```

VOLTAGE MATRIX
```
-5.831   -6.227   -5.165   -8.167   -4.043   -9.039   -2.564   -7.668   -0.8667  -3.104
 0.8818   3.428    2.510    8.195    3.861    9.170    4.815    7.664    5.300    5.350
 5.300    3.052    4.854    1.071    4.053   -0.4773   3.016   -1.548    1.847   -2.151
 0.4689  -2.277   -0.6028  -1.766   -0.9095  -0.9956  -0.6002  -0.3912   0.0      0.0
 0.0      0.0      0.0      0.0      0.0      0.0      0.0      0.0      0.0      0.0
 0.0      0.0      0.0      0.0      0.0      0.0      0.0      0.0      0.0      0.0
 0.0      0.0      0.0      0.0      0.0      0.0      0.0      0.0      0.0      0.0
 0.0      0.0      0.0      0.0      0.0      0.0
```

```
M1 N1    XR       XP       XZ       UR       UP       UZ
1 14     4.3615   0.0      5.3235   1.0000   0.0      0.0
```

VOLTAGE MATRIX
```
-0.3635   0.3747  -0.7094  -0.3021  -1.030   -1.361   -1.288   -2.289   -1.453   -1.891
-1.505    0.2609  -1.436    2.391   -1.254    3.052   -0.9794   2.764   -0.6430   2.299
-0.2827    1.903   0.6261E-01 1.563   0.3577   1.238    0.5755   0.9081   0.6301   0.6217
 0.1833    0.8129  -0.1351   1.507   0.2153E-01 2.204   0.3355    2.642   -3.390   -2.297
-1.780   -4.455    0.8802   -6.354   4.015    -7.719    6.202   -8.351    5.421   -8.158
 3.271   -7.168    0.4026E-03-5.529  -2.443   -3.479   -3.637   -1.311   -3.707    0.6757
-2.936    2.224   -1.646    3.159   -0.1624   3.438    1.213    3.014    2.231    2.147
 2.764    1.122    2.900    0.2504   2.855   -0.2988
```

```
M1 N1    XR       XP       XZ       UR       UP       UZ
2 14     4.3615   0.0      5.3235   1.0000   0.0      0.0
```

VOLTAGE MATRIX
```
-0.2404E-01-0.1175E-01-0.5851E-01-0.8933E-01-0.1031   -0.3228   -0.1544   -0.7218   -0.2078   -0.9031
-0.2570   -0.4097   -0.2995    0.2419   -0.3273    0.3980   -0.3383    0.2594   -0.3302    0.1377
-0.3035    0.9742E-01-0.2608    0.1062   -0.2058    0.1305   -0.1442    0.1508   -0.9805E-01 0.1466
-0.1815    0.7648E-01-0.2948    0.6018E-01-0.2884    0.9151E-01-0.1704    0.7544E-01 0.4761E-01-0.1454
 0.3126   -0.3597    1.098    -0.6309    2.504    -0.9261    4.105    -1.204    4.701    -1.423
 3.757    -1.545    2.166    -1.546    0.8333   -1.417   -0.4390E-01-1.168   -0.5635   -0.8291
-0.8229   -0.4407   -0.8812   -0.5229E-01-0.7814    0.2877   -0.5664    0.5365   -0.2864    0.6409
-0.3853E-01 0.5691   0.8371E-01 0.3899   0.7771E-01 0.1892
```

C. Program for Gain Patterns

```
//                  (0034,EE,6,2,,2),'MAUTZ,JOE',REGION=370K
// MSG T, PLEASE RUN WITH BLACK INK IN THE CALCOMP PLOTTER PEN
// EXEC FORTGCLG,PARM.FORT='MAP'
//FORT.SYSIN DD *
      SUBROUTINE PLANE(VVR,THR,NT)
      COMPLEX VVR(1),A5,A6,U
      COMMON U,R(42),ZS(42),SV(42),CV(42),BK,NP,NN,T(80),TR(80)
      DIMENSION BJ(126),THR(1),FK(20)
      KG=NP-1
      NM=KG/2-1
      M2=NN+2
      A5=2.*3.141593*U**(NM+1)
      NV=NM*4
      FK(1)=1.
      DO 153 J=1,M2
      J1=J+1
      FK(J1)=FK(J)*J
  153 CONTINUE
      DO 156 L=1,NT
      L1=(L-1)*NV
      CS=COS(THR(L))
      SN=SIN(THR(L))
      BCS=BK*CS
      DO 302 J=1,KG
      X=R(J)*BK*SN
      J1=J
      I1=NN
      IF(I1) 303,304,303
  304 I1=I1+1
      J1=J1+KG
  303 DO 305 JJ=I1,M2
      IF(X-1.E-5) 1,1,2
    1 IF(JJ-1) 3,3,4
    3 BJ(J1)=1.
      GO TO 306
    4 BJ(J1)=0.
      GO TO 306
    2 RH=X/2.
      RH2=RH*RH
      RH3=RH**(JJ-1)
      BJ(J1)=RH3/FK(JJ)
      SS=BJ(J1)
    8 SST=SS*1.E-7
      DO 155 K=1,20
      SS=-SS*RH2/K/(K+JJ-1)
      BJ(J1)=BJ(J1)+SS
      IF(ABS(SS)-SST) 306,306,155
  155 CONTINUE
      STOP 155
  306 J1=J1+KG
  305 CONTINUE
  302 CONTINUE
      IF(NN) 307,308,307
  308 DO 309 J=1,KG
      J1=J+2*KG
      BJ(J)=-BJ(J1)
  309 CONTINUE
  307 DO 300 J=1,NM
      J1=J+L1
      J2=J1+NM
```

```
                J3=J2+NM
                J4=J3+NM
                VVR(J1)=0.
                VVR(J2)=0.
                VVR(J3)=0.
                VVR(J4)=0.
                DO 301 I=1,4
                I1=2*(J-1)+I
                I4=4*(J-1)+I
                I2=I1+KG
                I3=I2+KG
                A6=(COS(ZS(I1)*BCS)+U*SIN(ZS(I1)*BCS))*A5
                BJ1=(BJ(I3)+BJ(I1))*.5
                BJ2=(BJ(I3)-BJ(I1))*.5
                VVR(J1)=VVR(J1)+A6*(CS*SV(I1)*BJ2+SN*CV(I1)*BJ(I2)*U)*T(I4)
                VVR(J2)=VVR(J2)+A6*CS*BJ1*U*TR(I4)
                VVR(J3)=VVR(J3)-A6*SV(I1)*BJ1*U*T(I4)
                VVR(J4)=VVR(J4)+A6*BJ2*TR(I4)
         301    CONTINUE
         300    CONTINUE
         156    CONTINUE
                RETURN
                END
                COMPLEXU,U1,U2,U3,U4,VR(22192),Y(5776),E(146),E1(146),V(38),TI(38)
                DIMENSION RH(43),ZH(43),DH(42),TH(145),KK1(10),S6(145),S7(145)
                DIMENSION E3(146),E4(146),AREA(400)
                COMMON U,R(42),ZS(42),SV(42),CV(42),BK,NP,NN,T(80),TR(80)
                ETA=376.730
                PI=3.141593
                U=(0.,1.)
                CALL PLOTS(AREA,400)
                REWIND 6
          88    READ(1,51,END=52) KV,NP,NMAX,NT,BK
          51    FORMAT(4I3,E14.7)
                WRITE(3,54) KV,NP,NMAX,NT,BK
          54    FORMAT(1X//' KV=',I3,' NP=',I3,' NMAX=',I3,' NT=',I3,' BK=',E14.7)
                READ(1,53)(RH(I),I=1,NP)
                READ(1,53)(ZH(I),I=1,NP)
          53    FORMAT(10F8.4)
                WRITE(3,55)
          55    FORMAT(1X/' RH')
                WRITE(3,46)(RH(I),I=1,NP)
          46    FORMAT(1X,10F8.4)
                WRITE(3,56)
          56    FORMAT(1X/' ZH')
                WRITE(3,46)(ZH(I),I=1,NP)
                KL=1
         126    IF((RH(1)-RH(NP)).NE.0..OR.(ZH(1)-ZH(NP)).NE.0.) GO TO 58
                KL=0
                RH(NP+1)=RH(2)
                ZH(NP+1)=ZH(2)
                RH(NP+2)=RH(3)
                ZH(NP+2)=ZH(3)
                NP=NP+2
          58    DO 57 I=2,NP
                I2=I-1
                RR1=RH(I)-RH(I2)
                RR2=ZH(I)-ZH(I2)
                DH(I2)=SQRT(RR1*RR1+RR2*RR2)
                R(I2)=.5*(RH(I)+RH(I2))
```

```
      7S(I2)=.5*(ZH(I)+ZH(I2))
      SV(I2)=RR1/DH(I2)
      CV(I2)=RR2/DH(I2)
   57 CONTINUE
      NM=(NP-3)/2
      NM2=NM*2
      NM4=NM*4
      N7=NM2*NM2
      NT2=NT*2
      NT3=NT+1
      DO 74 J=1,NM
      J2=2*(J-1)+1
      J3=J2+1
      J4=J3+1
      J5=J4+1
      J6=4*(J-1)+1
      J7=J6+1
      J8=J7+1
      J9=J8+1
      DEL1=DH(J2)+DH(J3)
      DEL2=DH(J4)+DH(J5)
      T(J6)=DH(J2)*DH(J2)/2./DEL1
      T(J7)=DH(J3)*(DH(J2)+DH(J3)/2.)/DEL1
      T(J8)=DH(J4)*(DH(J5)+DH(J4)/2.)/DEL2
      T(J9)=DH(J5)*DH(J5)/2./DEL2
   74 CONTINUE
      DO 75 J=1,NM4
      TR(J)=T(J)
   75 CONTINUE
  115 IF(KL.EQ.0) GO TO 78
      IF(RH(1)) 77,23,77
   77 DEL1=DH(1)+DH(2)
      TR(1)=DH(1)*(1.+(DH(2)+DH(1)/2.)/DEL1)
      TR(2)=DH(2)*(1.+DH(2)/2./DEL1)
   23 IF(RH(NP)) 79,78,79
   79 J1=(NM-1)*4+3
      J2=J1+1
      DEL2=DH(NP-2)+DH(NP-1)
      TR(J1)=DH(NP-2)*(1.+DH(NP-2)/2./DEL2)
      TR(J2)=DH(NP-1)*(1.+(DH(NP-2)+DH(NP-1)/2.)/DEL2)
   78 DEL=PI/(NT-1)
      DO 60 J=1,NT
      TH(J)=(J-1)*DEL
      S6(J)=COS(TH(J))
      S7(J)=SIN(TH(J))
   60 CONTINUE
      DO 61 J=1,NMAX
      NN=J-1
      J1=1+NM4*NT*(J-1)
  263 CALL PLANE(VR(J1),TH,NT)
      J2=(J-1)*NZ+1
      J3=J2+NZ-1
      READ(6)(Y(I),I=J2,J3)
      WRITE(3,254)
  254 FORMAT('0FIRST TWO ELEMENTS OF ADMITTANCE MATRIX')
      WRITE(3,25) Y(J2),Y(J2+1)
   25 FORMAT(1X,10G11.4)
   61 CONTINUE
      DO 62 K=1,KV
      READ(1,63) NX,(KK1(I),I=1,NX)
```

```
 63 FORMAT(10I3)
    READ(1,64) XR,XZ,UR,UP,UZ
 64 FORMAT(5F9.4)
    PIL=UR*UR+UZ*UZ+UP*UP
    P=BK*BK*ETA/6./PI*PIL
    P4=BK*SQRT(ETA/4./PI)
    WRITE(3,65) NX,(KK1(I),I=1,NX)
 65 FORMAT('0NX=',I3,' KK1=',8I3)
    WRITE(3,66)
 66 FORMAT('0',4X,'XR',7X,'XZ',7X,'UR',7X,'UP',7X,'UZ')
    WRITE(3,67) XR,XZ,UR,UP,UZ
 67 FORMAT(1X,5F9.4)
    J7=0
    IF(UP.NE.0.) J7=NM2
    DO 69 J=1,NT2
    E(J)=0.
 69 CONTINUE
    U2=0.
    DO 68 J=1,NX
    READ(1,72)(V(I),I=1,NM2)
 72 FORMAT(7E11.4)
    WRITE(3,73) KK1(J)
 73 FORMAT('0VOLTAGE MATRIX FOR THE EXP(J',I2,'0) MODE')
    WRITE(3,255)
255 FORMAT('+',30X,'/')
    WRITE(3,83)(V(I),I=1,NM2)
 83 FORMAT(1X,7E11.4)
248 NN=KK1(J)
    S=(-1.)**NN
    J3=NN*NZ
    DO 70 I=1,NM2
    TI(I)=0.
    DO 71 L=1,NM2
    L1=J3+(L-1)*NM2+I
    TI(I)=TI(I)+Y(L1)*V(L)
 71 CONTINUE
 70 CONTINUE
    DO 84 L=1,NT
    L2=L+NT
    DO 85 I=1,NM2
    L1=NN*NM4*NT+(L-1)*NM4+J7+I
    U1=VR(L1)*TI(I)
    E(L)=E(L)+U1
    E(L2)=E(L2)+S*U1
 85 CONTINUE
 84 CONTINUE
    IF(UP) 48,47,48
 47 U3=2.
    U4=2.*U
    S1=1.
    GO TO 45
 48 U3=2.*U
    U4=2.
    S1=-1.
 45 IF(NN.NE.0) GO TO 50
    U3=.5*U3
    U4=.5*U4
    S1=.5*S1
    DO 86 L=1,NT2
    E(L)=.5*E(L)
```

```
 86 CONTINUE
 50 DO 40 L=1,NM
    L1=L+NM
    E1(L)=TI(L)*U3
    E1(L1)=TI(L1)*U4
    E3(L)=CABS(E1(L))
    E3(L1)=CABS(E1(L1))
 40 CONTINUE
    WRITE(3,256)
256 FORMAT('OCURRENT')
    WRITE(3,25)(E1(L),L=1,NM2)
    WRITE(3,257)
257 FORMAT('OMAGNITUDE OF CURRENT')
    WRITE(3,25)(E3(L),L=1,NM2)
    U1=0.
    U3=0.
    DO 243 L=1,NM
    U1=U1+V(L)*TI(L)
    L2=L+NM
    U3=U3+V(L2)*TI(L2)
243 CONTINUE
    U2=U2-S1*(U1-U3)
 68 CONTINUE
    U2=U2*2.
264 P2=P4/SQRT(P+REAL(U2))
    U2=U2/PIL
    P=P/PIL
    WRITE(3,260) P,U2
260 FORMAT('ORADIATION RESISTANCE OF ISOLATED DIPOLE=',E11.4/' MUTUAL
   1IMPEDANCE=',2E11.4)
    DO 90 L=1,NT2
    E(L)=E(L)*2.
    E3(L)=CABS(E(L))
 90 CONTINUE
    WRITE(3,258)
258 FORMAT('OSCATTERED FAR ELECTRIC FIELD')
    WRITE(3,25)(E(L),L=1,NT,8)
    WRITE(3,25)(E(L),L=NT3,NT2,8)
    WRITE(3,25)(E3(L),L=1,NT,8)
    WRITE(3,25)(E3(L),L=NT3,NT2,8)
    S3=SQRT(XZ*XZ+XR*XR)
    S=ARCOS(XZ/S3)
    IF(UP) 93,92,93
 92 DO 87 J=1,NT
    J2=J+NT
    S2=UR*S6(J)-UZ*S7(J)
    S1=COS(TH(J)-S)*S3*BK
    E1(J)=S2*(COS(S1)+U*SIN(S1))
    S5=-UR*S6(J)-UZ*S7(J)
    S4=COS(TH(J)+S)*S3*BK
    E1(J2)=S5*(COS(S4)+U*SIN(S4))
 87 CONTINUE
    GO TO 94
 93 DO 95 J=1,NT
    J2=J+NT
    S1=COS(TH(J)-S)*S3*BK
    E1(J)=(COS(S1)+U*SIN(S1))*UP
    S4=COS(TH(J)+S)*S3*BK
    E1(J2)=(-COS(S4)-U*SIN(S4))*UP
 95 CONTINUE
```

```
  94 DO 96 J=1,NT2
     E1(J)=P2*(E1(J)+E(J))
     S1=CABS(E1(J))
     E3(J)=S1*S1
 250 IF(E3(J).GT.5.5) E3(J)=5.5
  96 CONTINUE
     WRITE(3,259)
 259 FORMAT('0GAIN')
     WRITE(3,25)(E3(J),J=1,NT,8)
     WRITE(3,25)(E3(J),J=NT3,NT2,8)
     DO 244 J=1,NT
     S1=E3(J)
     E3(J)=6.+S1*S7(J)
     E4(J)=5.+S1*S6(J)
     J1=J+NT
     S1=E3(J1)
     E3(J1)=6.-S1*S7(J)
     E4(J1)=5.+S1*S6(J)
 244 CONTINUE
 265 CALL LINE(E3(1),E4(1),NT,1,0,0)
 266 CALL LINE(E3(NT3),E4(NT3),NT,1,0,0)
     E3(1)=1.
     E3(2)=11.
     E3(3)=0.
     E3(4)=10.
     E4(1)=5.
     E4(2)=5.
     E4(3)=6.
     E4(4)=6.
 267 CALL LINE(E3(1),E4(1),2,1,0,0)
 268 CALL LINE(E4(3),E3(3),2,1,0,0)
     DO 245 J=1,11
     S1=J
     CALL SYMBOL(S1,5.,.14,13,0.,-1)
 245 CONTINUE
     DO 246 J=1,11
     S1=J-1
     CALL SYMBOL(6.,S1,.14,13,90.,-1)
 246 CONTINUE
 252 S1=5.96
     DO 253 J=1,5
     S1=S1+1.
     J1=J+112
     CALL SYMBOL(S1,5.1,.14,J1,0.,-1)
 253 CONTINUE
 261 CALL PLOT(11.,0.,-3)
  62 CONTINUE
     GO TO 88
  52 CALL PLOT(6.,0.,-3)
     STOP
     END
/*
//GO.FT06F001 DD DSNAME=EE0034.REV1,DISP=OLD,UNIT=2314,          X
//             VOLUME=SER=SU0004,DCB=(RECFM=V,BLKSIZE=1800,LRECL=1796)
//GO.SYSIN DD *
001041004073 0.4659995E+00
  0.0     0.0868  0.1736  0.2605  0.3473  0.4341  0.5209  0.6078  0.6946  0.7814
  0.8682  0.9551  1.0419  1.1287  1.2155  1.3024  1.3892  1.4760  1.5628  1.6497
  1.7365  1.8233  1.9101  1.9970  2.0838  2.1706  2.2574  2.3442  2.4311  2.5179
  2.6047  2.6837  2.6863  2.5969  2.4184  2.1570  1.8216  1.4238  0.9772  0.4971
```

```
  -0.0000
   0.0       0.4924    0.9848    1.4772    1.9696    2.4620    2.9544    3.4468    3.9392    4.4316
   4.9240    5.4164    5.9088    6.4013    6.8937    7.3861    7.8785    8.3709    8.8633    9.3557
   9.8481   10.3405   10.8329   11.3253   11.8177   12.3101   12.8025   13.2949   13.7873   14.2797
  14.7721   15.2657   15.7650   16.2562   16.7225   17.1478   17.5177   17.8195   18.0427   18.1798
  18.2260
004000001002003
     4.3615    5.3235    1.0000    0.0000    0.0000
-0.5831E 01-0.6227E 01-0.5165E 01-0.8167E 01-0.4043E 01-0.9039E 01-0.2564E 01
-0.7668E 01-0.8667E 00-0.3104E 01 0.8818E 00 0.3428E 01 0.2510E 01 0.8185E 01
 0.3861E 01 0.9170E 01 0.4815E 01 0.7664E 01 0.5300E 01 0.5350E 01 0.5300E 01
 0.3052E 01 0.4854E 01 0.1071E 01 0.4053E-01-0.4773E 00 0.3016E 01-0.1548E 01
 0.1847E 01-0.2151E 01 0.4689E 00-0.2277E 01-0.6028E 00-0.1766E 01-0.9095E 00
-0.9956E 00-0.6002E 00-0.3912E 00 0.0       0.0       0.0       0.0
 0.0       0.0       0.0       0.0       0.0       0.0       0.0
 0.0       0.0       0.0       0.0       0.0       0.0       0.0
 0.0       0.0       0.0       0.0       0.0       0.0       0.0
 0.0       0.0       0.0       0.0       0.0       0.0       0.0
 0.0       0.0       0.0       0.0       0.0       0.0
-0.3638E 00 0.3747E 00-0.7094E 00-0.3021E 00-0.1030E 01-0.1361E 01-0.1288E 01
-0.2289E 01-0.1453E 01-0.1891E 01-0.1505E 01 0.2609E 00-0.1436E 01 0.2391E 01
-0.1254E 01 0.3052E 01-0.9794E 00 0.2764E 01-0.6430E 00 0.2299E 01-0.2827E 00
 0.1903E 01 0.6261E-01 0.1563E 01 0.3577E 00 0.1238E 01 0.5755E 00 0.9081E 00
 0.6301E 00 0.6217E 00 0.1839E 00 0.8129E 00-0.1351E 00 0.1507E 01 0.2153E-01
 0.2204E 01 0.3355E 00 0.2642E-01-0.3390E 01-0.2297E 01-0.1789E 01-0.4455E 01
 0.8802E 00-0.6354E 01 0.4015E 01-0.7719E 01 0.6202F-01-0.8351E 01 0.5921E 01
-0.8158E 01 0.3273E 01-0.7168E 01 0.4026E-03-0.5529E 01-0.2443E 01-0.3479E 01
-0.3637E 01-0.1311E 01-0.3707E 01 0.6757E 00-0.2936E 01 0.2224E 01-0.1646E 01
 0.3159E 01-0.1624E 00 0.3408E 01 0.1213E 01 0.3014E 01 0.2231E 01 0.2147E 01
 0.2764E 01 0.1122E 01 0.2900E 01 0.2504E 00 0.2855E 01-0.2988E 00
-0.2404E-01-0.1175E-01-0.5851E-01-0.8933E-01-0.1031E 00-0.3228E 00-0.1544E 00
-0.7218E 00-0.2078E 00-0.9031E 00-0.2579E 00-0.4097E 00-0.2995E 00 0.2419E 00
-0.3273E 00 0.3980E 00-0.3383E 00 0.2594E 00-0.3302E 00 0.1377E 00-0.3036E 00
 0.9742E-01-0.2608E 00 0.1062E 00-0.2058E 00 0.1305E 00-0.1442E 00 0.1508E 00
-0.9805E-01 0.1466E 00-0.1815E 00 0.7648E-01-0.2948E 00 0.6018E-01-0.2884E 00
 0.9151E-01-0.1704E 00 0.7544E-01 0.4761E-01-0.1454E 00 0.3326E 00-0.3597E 00
 0.1098E 01-0.6309E 00 0.2504E 01-0.9261E 00 0.4105E 01-0.1204E 01 0.4701E 01
-0.1423E 01 0.3757E 01-0.1545E 01 0.2166E 01-0.1546E 01 0.8333E 00-0.1417E 01
-0.4390E-01-0.1168E 01-0.5635E 00-0.8291E 00-0.8229E 00-0.4407E 00-0.8812E 00
-0.5229E-01-0.7814E 00 0.2877E 00-0.5664E 00 0.5365E 00-0.2864E 00 0.6409E 00
-0.3853E-01 0.5691E 00 0.8371E-01 0.3899E 00 0.7771E-01 0.1892E 00
-0.3105E-03-0.7578E-03-0.1201E-02-0.7585E-02-0.2892E-02-0.4317E-01-0.5469E-02
-0.1431E 00-0.8912E-02-0.2367E 00-0.1305E-01-0.1274E 00-0.1762E-01 0.6862E-01
-0.2223E-01 0.1018E 00-0.2645E-01 0.3994E-01-0.2983E-01-0.6448E-02-0.3199E-01
-0.2235E-01-0.3263E-01-0.2171E-01-0.3162E-01-0.1489E-01-0.2901E-01-0.6747E-02
-0.2488E-01-0.1663E-02-0.2102E-01-0.1251E-01-0.1997E-01-0.2046E-01-0.1507E-01
-0.1421E-01-0.5823E-02-0.4817E-02 0.3772E-02-0.1788E-02 0.3112E-01-0.7132E-02
 0.1535E 00-0.1723E-01 0.5114E 00-0.3226E-01 0.1108E 01-0.5146E-01 0.1481E 01
-0.7307E-01 0.1241E 01-0.9452E-01 0.7248E 00-0.1128E 00 0.3403E 00-0.1251E 00
 0.1362E 00-0.1289E 00 0.3254E-01-0.1228E 00-0.2587E-01-0.1068E 00-0.6156E-01
-0.8211E-01-0.8178E-01-0.5145E-01-0.8812E-01-0.1837E-01-0.7648E-01 0.1055E-01
-0.4842E-01 0.2320E-01-0.2127E-01 0.1775E-01-0.5497E-02 0.6368E-02
/*
```

D. Sample Output (Plotter output is that of Figure 9a.)

KV= 1 NP= 41 NMAX= 4 NT= 73 BK= 0.4659995E 00

RH
```
( )     0.0868  0.1736  0.2605  0.3473  0.4341  0.5209  0.6078  0.6946  0.7814
0.8682  0.9551  1.0419  1.1287  1.2155  1.3024  1.3892  1.4760  1.5628  1.6497
1.7365  1.8233  1.9101  1.9970  2.0838  2.1706  2.2574  2.3442  2.4311  2.5179
2.6047  2.6837  2.6863  2.5969  2.4184  2.1570  1.8216  1.4238  0.9772  0.4971
0. )
```

ZH
```
0. )    0.4924  0.9848  1.4772  1.9696  2.4620  2.9544  3.4468  3.9392  4.4316
4.9240  5.4164  5.9088  6.4013  6.8937  7.3861  7.8785  8.3709  8.8633  9.3557
9.8481  10.3405 10.8329 11.3253 11.8177 12.3101 12.8025 13.2949 13.7873 14.2797
14.7721 15.2657 15.7650 16.2562 16.7225 17.1478 17.5177 17.8195 18.0427 18.1798
18.2260
```

FIRST TWO ELEMENTS OF ADMITTANCE MATRIX
0.2100E-04 0.9192E-04 0.4493E-04 0.5208E-04

FIRST TWO ELEMENTS OF ADMITTANCE MATRIX
0.2558E-05-0.2549E-02 0.4195E-05-0.2132E-02

FIRST TWO ELEMENTS OF ADMITTANCE MATRIX
0.9085E-06 0.1145E-04 0.6140E-06-0.2151E-02

FIRST TWO ELEMENTS OF ADMITTANCE MATRIX
0.4774E-05-0.3729E-02 0.3065E-05-0.5357E-02

NX= 4 KK1= 0 1 2 3

```
  KK        XZ        UR       UP       UZ
4.3015    5.3235    1.0000    0.0      0.0
```

VOLTAGE MATRIX FOR THE EXP(J 0*) MODE
```
-0.5431E 01-0.6227E 01-0.5165E 01-0.8167E 01-0.4043E 01-0.9039E 01-0.2564E 01
-0.7668E 01-0.8657E 00-0.3104E 01 0.8818E 00 0.3428E 01 0.2510E 01 0.8185E 01
 0.3361E 01 0.9170E 01 0.4815E 01 0.7664E 01 0.5300E 01 0.5350E 01 0.5301E 01
 0.3052E 01 0.4854E 01 0.1071E 01 0.4053E 01-0.4773E 00 0.3016E 01-0.1543E 01
 0.1847E 01-0.2151E 01 0.4689E 00-0.2277E 01-0.6028E 00 0.1766E 01-0.9095E 00
-0.9956E 00-0.6002E 00-0.3912E 00 0.0      0.0      0.0      0.0
 0.0      0.0      0.0      0.0      0.0      0.0      0.0
```

```
0.0      0.0      0.0      0.0      0.0      0.0      0.0
0.0      0.0      0.0      0.0      0.0      0.0      0.0
0.0      0.0      0.0      0.0      0.0      0.0      0.0
0.0      0.0      0.0      0.0      0.0      0.0
```

CURRENT
```
0.1229E-02-0.3952E-02 0.2734E-02-0.8094E-02 0.3619E-02-0.1038E-01 0.3126E-02-0.1012E-01 0.6791E-03-0.7146E-02
-0.3232E-02-0.1953E-02-0.6429E-02 0.4337E-02-0.3671E-02 0.1039E-01-0.3751E-02 0.1481E-01 0.1446E-02 0.1642E-01
 0.7395E-02 0.1469E-01 0.1260E-01 0.1037E-01 0.1582E-01 0.3478E-02 0.1625E-01-0.4317E-02 0.1366E-01-0.1145E-01
 0.7994E-02 0.1622E-01 0.1956E-02-0.1512E-01-0.7376E-03-0.8902E-02-0.4050E-04-0.2004E-02 0.0      0.0
 0.0      0.0      0.0      0.0      0.0      0.0      0.0      0.0      0.0      0.0
 0.0      0.0      0.0      0.0      0.0      0.0      0.0      0.0      0.0      0.0
 0.0      0.0      0.0      0.0      0.0      0.0      0.0      0.0      0.0      0.0
 0.0      0.0      0.0      0.0      0.0      0.0
```

MAGNITUDE OF CURRENT
```
0.4149E-02 0.8534E-02 0.1099E-01 0.1059E-01 0.7168E-02 0.3782E-02 0.7755E-02 0.1237E-01 0.1527E-01 0.1659E-01
0.1672E-01 0.1632E-01 0.1620E-01 0.1682E-01 0.1782E-01 0.1806E-01 0.1524E-01 0.8932E-02 0.2045E-02 0.0
0.0      0.0      0.0      0.0      0.0      0.0      0.0      0.0      0.0      0.0
0.0      0.0      0.0      0.0      0.0      0.0      0.0      0.0
```

VOLTAGE MATRIX FOR THE EXP(J 1Z) MODE
```
-0.3638E 00 0.3747E 00-0.7094E 00-0.3021E 00-0.1030E 01-0.1361E 01-0.1284E 01
-0.2289E 01-0.1453E 01-0.1891E 01-0.1505E 01 0.2609E 00-0.1436E 01 0.2391E 01
-0.1254E 01 0.3052E 01-0.9794E 00 0.2764E 01-0.6430E 00 0.2299E 01-0.2827E 00
 0.1703E 01 0.2261E-01 0.1563E 01 0.3577E 00 0.1238E 01 0.5755E 00 0.9081E 00
 0.6301E 00 0.6217E 00 0.1939E 00 0.8129E 00-0.1351E 00 0.1507E 01 0.2151E-01
 0.2220E 01 0.3355E 00 0.2642E 01-0.3350E 01-0.2297E 01-0.1789E 01 0.4455E 01
 0.8602E 00-0.6354E 01 0.4015E 01-0.7719E 01 0.6202E 01-0.8351E 01 0.5921E 01
-0.1159E 01 0.2273E 01-0.7169E 01 0.4029E 01-0.5529E 01 0.2443E 01 0.3471E 01
-0.3637E 01-0.1311E 01-0.3707E 01 0.6757E 00-0.2936E 01 0.2224E 01-0.1641E 01
 0.3159E 01-0.1624E 00 0.3408E 01 0.1213E 01 0.3014E 01 0.2231E 01 0.2147E 01
 0.2766E 01 0.1122E 01 0.2900E 01 0.2504E 00 0.2855E 01-0.2968E 00
```

CURRENT
```
-0.5432E-03-0.1700E-02 0.1494E-03-0.3251E-02 0.1939E-02-0.4473E-02 0.2641E-02-0.4050E-02 0.3796E-03-0.1755E-02
-0.3743E-02 0.1423E-02-0.4001E-02 0.5675E-02-0.9551E-02 0.1056E-01-0.6490E-02 0.1419E-01-0.1167E-02 0.1668E-01
 0.5809E-02 0.1693E-01 0.1268E-01 0.1450E-01 0.1778E-01 0.1075E-01 0.2019E-01 0.5164E-02 0.1988E-01-0.6943E-03
 0.1261E-01-0.6050E-02 0.3390E-02-0.7747E-02 0.2978E-02-0.5552E-02-0.3739E-02-0.2326E-02 0.1776E-03 0.3953E-03
-0.2088E-03 0.4420E-03-0.9385E-03 0.1705E-02-0.9029E-03 0.1988E-02-0.1144E-02 0.2690E-02-0.2370E-02 0.4011E-02
-0.8254E-03 0.3425E-02-0.5181E-03 0.3714E-02-0.9460E-03 0.4631E-02 0.2603E-02 0.2205E-02-0.6548E-03 0.4022E-02
 0.3123E-02 0.5137E-03-0.5651E-03 0.1849E-02 0.1748E-02-0.7704E-03-0.2094E-02-0.1044E-02-0.6902E-03-0.4162E-02
-0.4872E-02-0.5599E-02-0.4609E-02-0.5306E-02-0.4071E-02-0.2222E-02
```

MAGNITUDE OF CURRENT
```
 0.1689E-02 0.3255E-02 0.4875E-02 0.4830E-02 0.1796E-02 0.4053E-02 0.9810E-02 0.1424E-01 0.1561E-01 0.1672E-01
 0.1790E-01 0.1949E-01 0.2078E-01 0.2084E-01 0.1881E-01 0.1398E-01 0.8447E-02 0.6256E-02 0.4405E-02 0.3217E-03
 0.9649E-03 0.1946E-02 0.2183E-02 0.2924E-02 0.4659E-02 0.3518E-02 0.3750E-02 0.4727E-02 0.3409E-02 0.4075E-02
 0.3232E-02 0.1965E-02 0.1911E-02 0.2340E-02 0.4219E-02 0.7422E-02 0.7028E-02 0.4637E-02
```

VOLTAGE MATRIX FOR THE EXP(J 20) MODE
```
-0.2404E-01-0.1175E-01 0.5851E-01-0.8933E-01-0.1031E 00-0.3228E 00-0.1544E 00
-0.7219E 00-0.2078E 00-0.9031E 00-0.2579E 00-0.4097E 00-0.2995E 00 0.2419E 00
-0.3274E 00 0.3980E 00-0.3383E 00 0.2594E 00-0.3302E 00 0.1377E 00-0.3036E 00
 0.9742E-01-0.2608E 00 0.1062E 00-0.7058E 00 0.1305E 00-0.1442E 00 0.1508E 00
-0.9805E-01 0.1466E 00 0.1815E 00 0.7648E-01-0.2948E 00 0.6018E-01-0.2884E 00
 0.9151E-01-0.1704E 00 0.7544E-01 0.4761E-01-0.1454E 00 0.3326E 00-0.3597E 00
 0.1099E-01-0.6309E 00 0.2504E-01-0.9261E 00 0.4105E-01-0.1204E 01 0.4701E 01
-0.1423E 01 0.3757E 01-0.1545E 01 0.2166E 01-0.1546E 01 0.8333E 00-0.1417E 01
-0.4490E-01-0.1168E 01-0.5635E 00-0.8291E 00-0.8229E 00-0.4407E 00-0.8812E 00
-0.5229E-01-0.7814E 00 0.2877E 00-0.5664E 00 0.5365E 00-0.2864E 00 0.6409E 00
```



```
-0.3855E-01 0.5691E 00 0.8371E-01 0.3899E 00 0.7771E-01 0.1892E 00
```

CURRENT
```
-0.3152E-03 0.1554E-03-0.3951E-04 0.4415E-05 0.7514E-03-0.3793E-03 0.1171E-02-0.4804E-03 0.6044E-03-0.9956E-04
-0.7845E-03 0.2922E-03-0.2578E-02 0.5554E-03-0.4128E-02 0.1343E-02-0.4394E-02 0.2586E-02-0.3493E-02 0.3376E-02
-0.2693E-02 0.3949E-02-0.1576E-02 0.4681E-02 0.2492E-03 0.4573E-02 0.1432E-02 0.3822E-02 0.2387E-02 0.2994E-02
 0.3185E-02 0.1153E-02 0.2213E-02-0.4928E-03 0.8858E-03-0.5836E-03 0.4080E-03-0.1923E-03 0.2361E-04-0.1105E-04
-0.1093E-03 0.6760E-04-0.2954E-03 0.1572E-03-0.4028E-03 0.1160E-03-0.7932E-03 0.1283E-03-0.1471E-02 0.4770E-03
-0.1377E-02 0.7002E-03-0.9449E-03 0.3946E-03-0.1246E-02 0.5081E-03-0.8836E-03 0.1091E-02 0.2174E-03 0.5914E-03
-0.3192E-03-0.2435E-03-0.2096E-03 0.1045E-02 0.1218E-02 0.1530E-02 0.1956E-02-0.1562E-03 0.1386E-02 0.6704E-03
 0.2543E-02-0.7845E-03 0.5452E-03-0.8310E-03 0.1963E-03-0.1068E-03
```

MAGNITUDE OF CURRENT
```
 0.3515E-03 0.3976E-04 0.8417E-03 0.1266E-02 0.6126E-03 0.8373E-03 0.2637E-02 0.4341E-02 0.5099E-02 0.4858E-02
 0.4773E-02 0.4439E-02 0.4580E-02 0.4082E-02 0.3829E-02 0.3387E-02 0.2267E-02 0.1061E-02 0.4510E-03 0.2606E-04
 0.1290E-03 0.3347E-03 0.4191E-03 0.8035E-03 0.1546E-02 0.1545E-02 0.1024E-02 0.1345E-02 0.1404E-02 0.6301E-03
 0.4145E-02 0.1065E-02 0.1228E-02 0.2503E-02 0.1540E-02 0.2661E-02 0.9939E-03 0.2235E-03
```

VOLTAGE MATRIX FOR THE EXP(J 30) MODE
```
-0.3110E-03-0.7578E-03-0.1291E-02-0.7585E-02-0.2892E-02-0.4317E-01-0.5469E-02
-0.1443E 00-0.8912E-02-0.2367E 00-0.1305E-01-0.1274E 00-0.1762E-01 0.6862E-01
-0.2220E-01 0.1018E 00-0.2645E-01 0.3994E-01-0.2983E-01-0.6448E-02-0.3199E-01
-0.2239E-01-0.4263E-01-0.2171E-01-0.3162E-01-0.1489E-01-0.2921E-01-0.6747E-02
-0.2484E-01-0.1653E-02-0.2102E-01-0.1251E-01-0.1997E-01-0.2046E-01-0.1507E-01
-0.1421E-01-0.5823E-02-0.4817E-02 0.3772E-02-0.1788E-02 0.3112E-01-0.7132E-02
 0.1635E 00-0.1723E-01 0.5114E 00-0.3226E-01 0.1108E 01-0.5146E-01 0.1481E 01
-0.7307E-01 0.1241E-01-0.9452E-01 0.7248E 00-0.1128E 00 0.3403E 00-0.1251E 00
 0.1362E 00-0.1249E 00 0.3254E-01-0.1228E 00-0.2587E-01-0.1068E 00-0.6156E-01
-0.8911E-01-0.6178E-01-0.5145E-01-0.8812E-01-0.1837E-01-0.7648E-01 0.1055E-01
-0.4842E-01 0.2320E-01-0.2127E-01 0.1775E-01-0.5497E-02 0.6358E-02
```

CURRENT
```
 0.2153E-04-0.3158E-04 0.2073E-04-0.2002E-04 0.2064E-04 0.1999E-04 0.7736E-04 0.2411E-04 0.1441E-03-0.1865E-04
-0.5531E-04-0.2932E-04-0.6464E-03 0.3848E-04-0.1151E-02 0.1126E-03-0.1056E-02 0.1354E-03-0.6867E-03 0.1963E-03
-0.7117E-03 0.7442E-03-0.7900E-03 0.4493E-03-0.3773E-03 0.4744E-03-0.9894E-04 0.5371E-03-0.2156E-03 0.5705E-03
 0.6214E-04 0.4241E-03 0.3606E-03 0.1900E-03 0.2677E-04 0.4043E-04-0.2062E-03-0.2548E-05-0.1125E-05 0.1625E-05
 0.9587E-06-0.3694E-05-0.8477E-05-0.5289E-05-0.6713E-04 0.9269E-05-0.2144E-03 0.2335E-04-0.3444E-03 0.1032E-04
-0.2608E-03-0.2159E-05-0.2389E-03 0.3523E-04-0.4040E-03 0.7426E-04-0.2449E-03 0.3809E-04-0.1260E-03 0.1724E-04
-0.8152E-04 0.9512E-14-0.3535E-03 0.1010E-03 0.1627E-03 0.1184E-04 0.2343E-03 0.8475E-04-0.3397E-03 0.2046E-03
 0.1599E-03 0.1402E-03-0.3046E-03 0.4123E-04-0.5872E-04-0.1922E-06
```

MAGNITUDE OF CURRENT
```
 0.3830E-04 0.2846E-04 0.2873E-04 0.8103E-04 0.1453E-03 0.6376E-04 0.6475E-03 0.1156E-02 0.1064E-02 0.7142E-03
 0.7206E-03 0.5001E-03 0.6061E-03 0.5461E-03 0.6099E-03 0.4297E-03 0.4075E-03 0.4849E-03 0.2062E-03 0.1976E-05
 0.3792E-05 0.5991E-05 0.6777E-04 0.2156E-03 0.3446E-03 0.2608E-03 0.2415E-03 0.4108E-03 0.2478E-03 0.1271E-03
 0.1253E-03 0.3676E-04 0.1627E-03 0.2492E-03 0.3966E-03 0.2126E-03 0.3073E-03 0.5872E-04
```

RADIATION RESISTANCE OF ISOLATED DIPOLE= 0.4340E 01
MUTUAL IMPEDANCE= 0.7874E 00-0.2065E 00

SCATTERED FAR ELECTRIC FIELD
```
-0.4735E-01 0.1069     -0.3992      0.2280     -0.2857      0.6205      0.3594      0.4513      0.1416     -0.1692
-0.2010      0.1059      0.1740E-01 0.2341      0.6947E-01 0.1291      0.2284E-01 0.8678E-01-0.6737E-01 0.4366E-01
 0.4735E-01-0.1069     -0.3716      0.9929E-01-0.1102      0.6543      0.5765     -0.2928E-01-0.4798     -0.2546
-0.2727E-01 0.4424     -0.2427E-01 0.7583E-01 0.2546E-01 0.2793      0.1714      0.1002      0.6737E-01-0.4366E-01
 0.1069      0.4597      0.4831      0.5769      0.2206      0.2277      0.2347      0.1466      0.8973E-01 0.8028E-01
 0.1169      0.3846      0.6675      0.5773      0.5432      0.4432      0.7961E-01 0.2805      0.1585      0.8028E-01
```

GAIN
```
 1.549      2.394      1.814      0.3687     0.4117E-02 0.5696E-01 0.2202      0.8009      1.342      1.211
 1.549      1.015      0.7717     0.8673E-01 0.3006      0.1697      0.3424      0.8310      0.7374      1.211
```

VIII. REFERENCES

(1) J. Van Bladel, "Electromagnetic Fields," McGraw-Hill Book Co., New York, 1964, pp. 16-18.

(2) R. F. Harrington and J. R. Mautz, "Computation of Radiation and Scattering from Loaded Bodies of Revolution," Interaction Note 189, January 1970.

(3) R. F. Harrington, "Field Computation by Moment Methods," Macmillan Co., New York, 1968.

(4) R. F. Harrington and J. R. Mautz, "Radiation and Scattering from Bodies of Revolution," Interaction Note 188, July 1969.

(5) R. F. Harrington, "Time-Harmonic Electromagnetic Fields," McGraw-Hill Book Co., New York, 1961, p. 340 and p. 292.

(6) J. R. Mautz and R. F. Harrington, "Generalized Network Parameters for Bodies of Revolution", Interaction Note 187, May 1968.